## REFERENCES


[1] De Jong, K.P. and Geus, J.W. Carbon Nanofibers: Catalytic Synthesis and Applications. **Catalysis Reviews - Science and Engineering** 42 (2000): 481-510.

[2] Kresge, C.T.; Leonowicz, M.E. and Vartuli J.C. Ordered mesoporous molecular sieves synthesized by a liquid-crystal template mechanism. **Nature** 359(1992): 710-712.

[3] Beck, J.S.; Vartuli, J.C. and Roth, W.J. A new family of mesoporous molecular sieves prepared with liquid crystal templates. **Journal of the American Chemical Society** 114 (1992): 10834-10843.

[4] Zhao, Xiu S.; Lu, G.Q. (Max), and Millar, Graeme J. Advance in Mesoporous Molecular Sieve MCM-41. **Industrial and Engineering Chemistry Research.** 35 (1996): 2075-2090.

[5] Reb, A. And Alt, H.G. Diastereomeric amido functionalized ansa half-sandwich complexes of titanium and zirconium as catalyst precursors for ethylene polymerization to give resins with bimodal molecular weight distributions. **Journal of Molecular Catalysis A: Chemical** 174 (2001): 35-49.

[6] Kim, J.D. and Soares, J.B.P. Copolymerization of ethylene and α-olefins with combined metallocene catalysts III. Production of polyolefins with controlled microstructures. **Journal of Polymer Science, Part A: Polymer Chemistry** 38 (2000): 1427-1432.

[7] Wang, Q.; Yang, H.X. and Fan, Z.Q. **Macromolecular Rapid Communications**. 23 (2002): 639.

[8] Smedberg, A.; Hjertberg, T. and Gustafsson, B. Characterization of an unsaturated low-density polyethylene. **Journal of Polymer Science, Part A: Polymer Chemistry** 41 (2003): 2974-2984.

[9] Natta, G. and Plno, P. Crystalline high polymers of α-olefins. **Journal of the American Chemical Society** 77 (1955): 1708-1710.

[10] Gambarotta, S. Coord. Vanadium-based Ziegler-Natta: Challenges, promises, problems. **Coordination Chemistry Reviews** 237 (2003): 229-243.

[11] Ma, Y.; Reardon, D.F. and Yap, G.P.A. **Organometallics** 18 (1999): 2773-2781.

[12] Kashiwa, N. The discovery and progress of $MgCl_2$-supported $TiCl_4$ catalysts. **Journal of Polymer Science, Part A: Polymer Chemistry** 42 (2004): 1-8.

[13] Kissin, Y.V. Multicenter nature of titanium-based Ziegler-Natta catalysts: Comparison of ethylene and propylene polymerization reactions. **Journal of Polymer Science, Part A: Polymer Chemistry** 41 (2003): 1745-1758.

[14] Hlatky, G. Heterogeneous single-site catalysts for olefin polymerization. **Chemical Reviews** 100 (2000): 1347-1376.

[15] Breslow, D. S. and Newburg, N. R. **Journal of the American Chemical Society**. 79 (1957): 5072-5073.

[16] Natta, G.; Pino, P. and Mazzanti, G. A crystallizable organometallic complex containing titanium and aluminum. **Journal of the American Chemical Society** 79 (1957): 2975-2976.

[17] Sinn, H. and Kaminsky, W. **Adv. Organomet. Chem.** 18 (1980): 99-149

[18] Arlman, E.J. and Cossee, P. **Journal of Catalysis** 3 (1964): 99-104.

[19] Chung, T.-C.and Xu, G. US 6248837 B1, 2001 assigned to **The Penn State Research Foundation.**

[20] Fujita, M.; Seki, Y. and Miyatake, T. Synthesis of Ultra-High-Molecular-Weight Poly(α-olefin)s by Thiobis(phenoxy)titanium/Modified Methylaluminoxane System. **Journal of Polymer Science, Part A: Polymer Chemistry** 42 (2004): 1107-1111.

[21] Kashiwa, N. and Imuta, J. Recent progress on olefin polymerization catalysts. **Catalysis Surveys from Japan** 1 (1997): 125-142.

[22] Sinclair, K. B. and Wilson, R. B. **Chemistry & Industry** 7 (1994): 857-862.

[23] Gupta, V. K.; Satish, S. and Bhardwaj, I. S. Metallocene complexes of group 4 elements in the polymerization of monoolefins. **Journal of Macromolecular Science - Reviews in Macromolecular Chemistry and Physics** C34, No.3 (1994): 439-514.

[24] Naga, N. and Imanishi, Y. Copolymerization of ethylene and cyclopentene with zirconocene catalysts: Effect of ligand structure of zirconocenes. **Macromolecular Chemistry and Physics** 203 (2002: 159-165.

[25] Lauher, J. W. and Hoffmann, R. Structure and chemistry of bis(cyclopentadienyl)-MLn complexes. **Journal of the American Chemical Society**. 98 (1976): 1729-1742.

[26] Castonguay, L. A.and Rappe, A. K. Ziegler-Natta catalysis. A theoretical study of the isotactic polymerization of propylene. **Journal of the American Chemical Society**. 114 (1992): 5832-5842.

[27] Kaminsky, W. and Laban, A. Metallocene catalysis. **Applied Catalysis A: General** 222 (2001): 47-61.

[28] Yang, X.; Stern, C. L. and Marks,T. J. "Cation-like" homogeneous olefin polymerization catalysts based upon zirconocene alkyls and tris(pentafluoropnenyl)borane. **Journal of the American Chemical Society.** 113 (1991): 3623-3625.

[29] Chien, J. C. W. and Wang, B. P **Journal of Polymer Science Part A: Polymer Chemistry.** 26 (1988): 3089-3102.

[30] Pedeutour, J. N.; Radhakrishnan, K.; Cramail, H. and Deffieux, A. Use of "TMA-depleted" MAO for the activation of zirconocenes in olefin polymerization. **Journal of Molecular Catalysis A: Chemical.** 185 (2002): 119-125.

[31] Pedeutour, J. N.; Cramail, H. and Deffieux, A. Influence of X ligand nature in the activation process of racEt$(Ind)_2ZrX_2$ by methylaluminoxane. **Journal of Molecular Catalysis A: Chemical** 176 (2001): 87-94.

[32] Cam, D. and Giannini, U. **Makromolecular Chemistry** 193 (1992): 1049-1055.

[33] Soga, K.; Kim, H. J. and Shiono, T. **Macromolecular Rapid Communications.** 14 (1993): 765-770.

[34] Katayama, H.; Shiraishi, H.; Hino, T.; Ogane, T., and Imai, A. The effect of aluminum compounds in the copolymerization alpha - olefins. **Macromolecular Symposia** 97 (1995): 109-118.

[35] Przybyla, C.; Tesche, B., and Fink, G. Ethylene hexene copolymerization with the heterogeneous catalyst system $SiO_2$/MAO/rac-$Me_2$Si[2-Me-4-Ph-Ind](2)$ZrCl_2$: The filter effect. **Macromolecular Rapid Communications** 20 (1999): 328-332.

[36] Harkki, O.; Lehmus, P.; Leino, R.; Luttikhedde, H. J. G.; Nasman, J. H. and Seppala, J. V. Copolymerization of ethylene with 1-hexene or 1- hexadecane over siloxy-substituted metallocene catalysts. **Macromolecular Chemistry and Physics** 200 (1999): 1561-1565.

[37] Cheruvu, S. **US Pat 5608019** (1997).

[38] Albano, C.; Sánchez, G., and Ismayel, A. Influence of a copolymer on the mechanical properties of a blend of PP and recycled and non-recycled HDPE. **Polymer Bulletin** 41 (1998): 91-98.

[39] Shan, C. L. P.; Soares, J. B. P.; and Penlidis, A. Ethylene/ 1-octene copolymerization studies with in situ supported metallocene catalysts: Effect of polymerization parameters on the catalyst activity and polymer microstructure. **Journal of Polymer Science Part A: Polymer Chemistry** 40 (2002): 4426-4451.

[40] Pietikainen, P. and Seppala, J.V. Low molecular weight ethylene/propylene copolymers. Effect of process parameters on copolymerization with homogeneous $Cp_2ZrCl_2$ catalyst. **Macromolecules** 27 (1994): 1325-1328.

[41] Soga, K. and Kaminaka, M. **Macromolecular Rapid Communications** 13 (1992): 221-224.

[42] Nowlin, T. E.; Kissin, Y. V. and Wagner, K. P. High activity Ziegler-Natta catalysts for the preparation of ethylene copolymers. **Journal of Polymer Science Part A: Polymer Chemistry** 26 (1988): 755-764.

[43] Chu, K. J.; Soares, J. B. P. and Penlidis, A. Variation of molecular weight distribution (MWD) and short chain branching distribution (SCBD) of ethylene/ 1-hexene copolymers produced with different in-situ supported metallocene catalysts **Macromolecular Chemistry and Physics** 201 (2000): 340-348.

[44] Soga, K.; Uozumi, T.; Arai, T. and Nakamura, S. **Macromolecular Rapid Communications** 16 (1995): 379-385.

[45] De Fatima V. ; Marques, M. ; Conte, A., ; De Resende, F. C. and Chaves, E. G. Copolymerization of ethylene and 1-octene by homogeneous and different supported metallocenic catalysts. **Journal of Applied Polymer Science** 82 (2001): 724-730.

[46] Kim, J. D. and Soares, J. B. P. Copolymerization of ethylene and 1-hexene with supported metallocene catalysts: Effect of support treatment. **Macromolecular Rapid Communications** 20 (1999): 347-350.

[47] Chu, K. J.; Soares, J. B. P. and Penlidis, A. Polymerization mechanism for in situ supported metallocene catalysts. **Journal of Polymer Science Part A: Polymer Chemistry** 38 (2000): 462-468.

[48] Chu, K. J.; Soares, J. B. P. and Penlidis, A. Copolymerization of ethylehe and 1-hexene with in-situ supported $Et[Ind]_2ZrCl_2$. **Macromolecular Chemistry and Physics**. 200 (1999): 2372-2376.

[49] Shan, C. L. P.; Chu, K. J.; Soares, J., and Penlidis, A. Using alkylaluminium activators to tailor short chain branching distributions of ethylene/ 1-hexene copolymers produced with in-situ supported metallocene catalysts. **Macromolecular Chemistry and Physics** 201 (2000): 2195-2202.

[50] Kashiwa, N. and Imuta, J. Recent progress on olefin polymerization catalysts. **Catalysis Surveys from Japan** 1 (1997): 125-142.

[51] Sinclair, K. B. and Wilson, R. B. Chemistry & Industry 7 (1994): 857-862.

[52] Gupta, V. K.; Satish, S. and Bhardwaj, I. S. Metallocene complexes of group 4 elements in the polymerization of monoolefins. **Journal of Macromolecular Science - Reviews in Macromolecular Chemistry and Physics** C34, No.3 (1994): 439-514.

[53] Kaminsky, W. and Laban, A. Metallocene catalysis. **Applied Catalysis A: General** 222 (2001): 47-61.

[54] Naga, N. and Imanishi, Y. Copolymerization of ethylene and cyclopentene with zirconocene catalysts: Effect of ligand structure of zirconocenes. **Macromolecular Chemistry and Physics** 203 (2002): 159-165.

[55] Steinmetz, B.; Tesche, B.; Przybyla, C.; Zechlin, J. and Fink, G. Polypropylene growth on silica-supported metallocene catalysts: A microscopic study to explain kinetic behavior especially in early polymerization stages . **Acta Polymerica** 48 (1997): 392-399.

[56] Tait, P. J. T. and Monterio, M. G. K. **Mecton'96**, Houston, TX, USA June (1996).

[57] Quijada, R.; Rojas, R.; Alzamora, L.; Retuert, J. and Rabagliati, F. M. Study of metallocene supported on porous and nonporous silica for the polymerization of ethylene .**Catalysis letters** 46 (1997): 107-112.

[58] Chen, Y. X.; Rausch, M. D. and Chein, J. C. W. **Journal of Polymer Science Part A: Polymer Chemistry.** 33 (1995): 2093-2108.

[59] Ban, H.; Arai, T.; Ahn, C. H.; Uozumi, T. and Soga, T. **Recent Development in Heterogeneous Metallocene Catalyst**.

[60] Ferreira, M. L., Belelli, P. G., Juan, A., and Damiani, D. E. Theoretical and experimental study of the interaction of methylaluminoxane (MAO)-low temperature treated silica: Role of trimethylaluminium (TMA) **Macromolecular Chemistry and Physics** 201 (2000): 1334-1344.

[61] Collins, S.; Kelly, W. M. and Holden, D.A. Polymerization of propylene using supported, chiral, ansa-metallocene catalysts: Production of polypropylene with narrow molecular weight distributions. **Macromolecules** 25 (1992): 1780-1785.

[62] Kaminsky, W.; Renner, F. and Winkelbach, H. **Mecton'94**, Houston, TX, USA, May (1994).

[63] Hlatky. G. G. and Upton, D. J. Supported ionic metallocene polymerization catalysts. **Macromolecules** 29 (1996): 8019-8020.

[64] Lee, D. H.; Shin, S. Y. and Lee, D. H. Ethylene polymerization with metallocene and trimethylaluminum-trerated silica. **Macromolecular Symposia** 97 (1995): 195-203.

[65] Dos Santos, J. H. Z.; Dorneles, S.; Stedile, F.; Dupont, J.; Forte, M. M. C. and Baumovl, I. J. R. Silica supported zirconocenes and Al-based cocatalysts: Surface metal loading and catalytic activity **Macromolecular Chemistry and Physics** 198 (1997): 3529-3537.

[66] Harrison, D.; Coulter, I. M.; Wang, S.; Nistala, S.; Kuntz, B. A.; Pigeon, M.; Tian, J. and Collins. S. Olefin polymerization using supported metallocene catalysts: Development of high activity catalysts for use in slurry and gas phase ethylene polymerizations **Journal of Molecular Catalysis A: Chemical.** 128 (1998): 65-77.

[67] Xu, J.; Deng, Y.; Feng, L.; Cui, C. and Chen, W. Temperature rising elution fractionation of syndiotactic polypropylene prepared by homogeneous and supported metallocene catalysts **Polymer Journal** 30 (1998): 824-827.

[68] Soga, K.; Kim, H. J. and Shiono, T. **Macromolecular Rapid Communications.** 15 (1994): 139-144.

[69] Lee, D.; Yoon, K. and Noh, S. Polymerization of ethylene by using zirconocene catalyst anchored on silica with trisiloxane and pentamethylene spacers. **Macromolecular Rapid Communications** 18 (1997): 427-431.

[70] Iiskola, E. I.; Timonen, S.; Pakkanen, T. T.; Harkki, O.; Lehmus, P. and Seppala, J. V. Cyclopentadienyl surface as a support for zirconium polyethylene catalysts. **Macromolecules** 30 (1997) 2853-2859.

[71] Lee, D. and Yoon, K. **Macromolecular Symposia.** 97 (1995): 185-193.

[72] De Fatima V.; Marques, M.; Henriques, C. A.; Monteiro, J. L. F.; Menezes, S. M. C. and Coutinho, F. M. B. Ethylene polymerization with $Cp_2ZrCl_2$ supported on dealuminated Y zeolite **Polymer Bulletin.** 39 (1997): 567-571.

[73] Michelotti, M.; Altomare, A.; Ciardelli, F. and Roland, E. Zeolite supported polymerization catalysts: Copolymerization of ethylene and α-olefins with metallocenes supported on HY zeolite **Journal of Molecular Catalysis A: Chemical** 129 (1998): 241-248.

[74] Meshkova, I. N.; Ushakova, T. M.; Ladygina, T. A.; Kovalena, N. Y. and Novokshonova, L. A. Ethylene polymerization with catalysts on the base of Zr-cenes and methylaluminoxanes synthesized on zeolite support **Polymer Bulletin** 44 (2000): 461-468.

[75] Weiss, K.; Wirth-Pfeifer, C.; Hofmann, M.; Botzenhardt, S.; Lang, H.; Bruning, K. and Meichel, E. Polymerisation of ethylene or propylene with heterogeneous metallocene catalysts on clay minerals **Journal of Molecular Catalysis A: Chemical** 182-183 (2002): 143-149.

[76] Looveren, L. K. V.; Geysen, D. F.; Vercruysse, K. A.; Wouters, B. H.; Grobet, P. J. and Jacobs, P. A. Methylalumoxane MCM-41 as Support in the Co-Oligomerization of Ethene and Propene with [{$C_2H_4$(1-indenyl)$_2$} Zr($CH_3$)$_2$]. **Angewandte Chemie (International Edition in English)** 37 (1998): 517-520.

[77] Hagimoto, H.; Shiono, T. and Ikeda, T. Supporting effects of methylaluminoxane on the living polymerization of propylene with a chelating (diamide) dimethyltitanium complex. **Macromolecular Chemistry and Physics** 205 (2004): 19-26.

[78] B. Jongsomjit ; P. Kaewkrajang, S.E. Wanke and P. Praserthdam, A comparative study of ethylene/α-olefin copolymerization with silane-modified silica-supported MAO using zirconocene catalysts. **Catalysis Letters** 94 (2004): 205-208.

[79] B. Jongsomjit ; S. Ngamposri and P. Praserthdam, Role of titania in $TiO_2$-$SiO_2$ mixed oxides-supported metallocene catalyst during ethylene/1-octene copolymerization **Catalysis Letters** 100 (2005): 139-146.

[80] B. Jongsomjit ; S. Ngamposri and P. Praserthdam, Catalytic activity during copolymerization of ethylene and 1-hexene via mixed $TiO_2$/$SiO_2$-supported MAO with rac-Et[Ind] 2ZrCl2 metallocene catalyst **Molecules** 10 (2005): 672-678.

[81] B. Jongsomjit ; J. Panpranot and J.G. Goodwin, Jr., Co-support compound formation in alumina-supported cobalt catalysts **Journal of Catalysis.** 204 (2001): 98-109.

[82] B. Jongsomjit and J.G. Goodwin, Jr., Co-support compound formation in Co/$Al_2O_3$ catalysts: Effect of reduction gas containing CO. **Catalysis. Today** 77 (2002): 191-204.

[83] B. Jongsomjit ; J. Panpranot and J.G. Goodwin, Jr., Effect of zirconia-modified alumina on the properties of Co/γ -Al2O3 catalysts **Journal of Catalysis**. 215 (2003): 66-77.

[84] B. Jongsomjit ; C. Sakdamnuson and P. Praserthdam, Co-support compound formation in titania-supported cobalt catalyst **Catalysis Letters** 94 (2004): 209-215.

[85] T. Wongsalee ; B. Jongsomjit, P. Praserthdam, Effect of zirconia-modified titania consisting of different phases on characteristics and catalytic properties of Co/TiO2 catalysts **Catalysis Letters** 108 (2006): 55-61.

[86] B. Jongsomjit ; S. Ngamposri and P. Praserthdam, Application of silica/titania mixed oxide-supported zirconocene catalyst for synthesis of linear low-density polyethylene. **Industrial and Engineering Chemistry Research**. 44 (2005): 9059-9063.

[87] J.C. Randall **Journal of Macromolecular Science - Reviews in Macromolecular Chemistry and Physics**. C29 (1989): 201.

# APPENDICES

# APPENDIX A
# (Gel permeation chromatography)

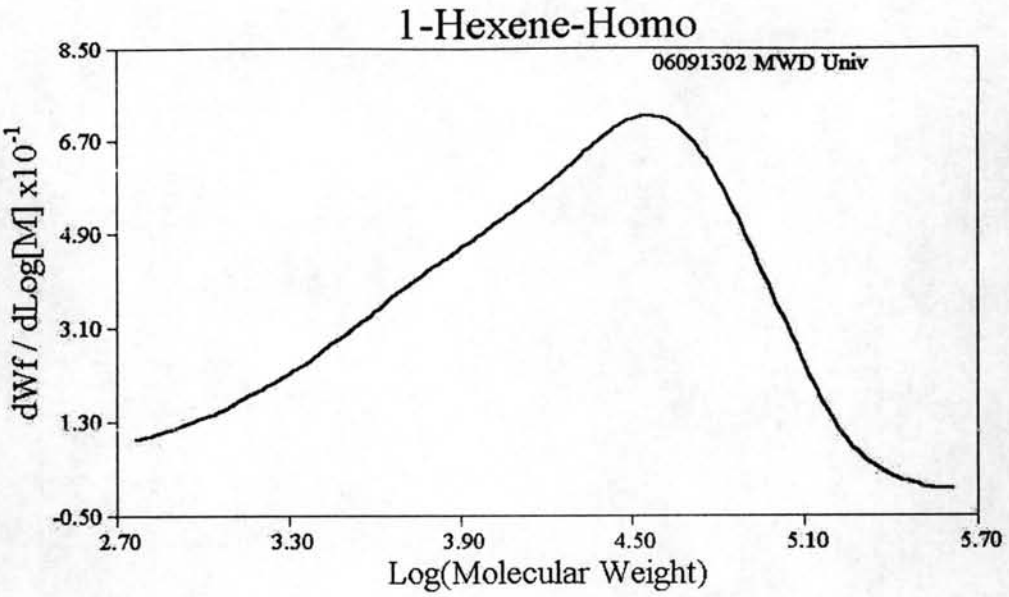


**Figure A-1** GPC curve of ethylene/1-hexene copolymer produce with homogenous

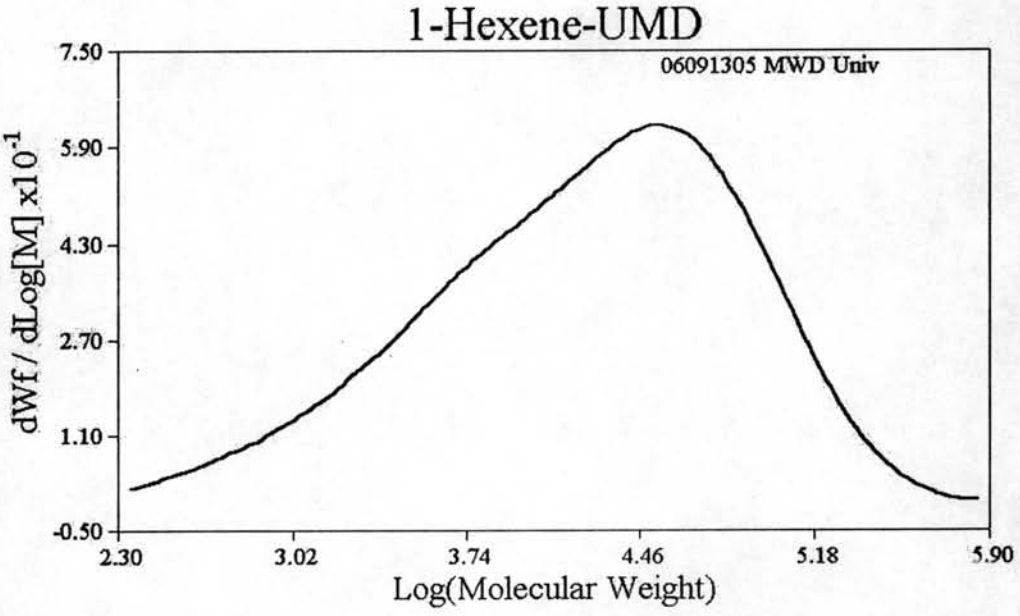


**Figure A-2** GPC curve of ethylene/1-hexene copolymer produce with MCM-41(UMD)

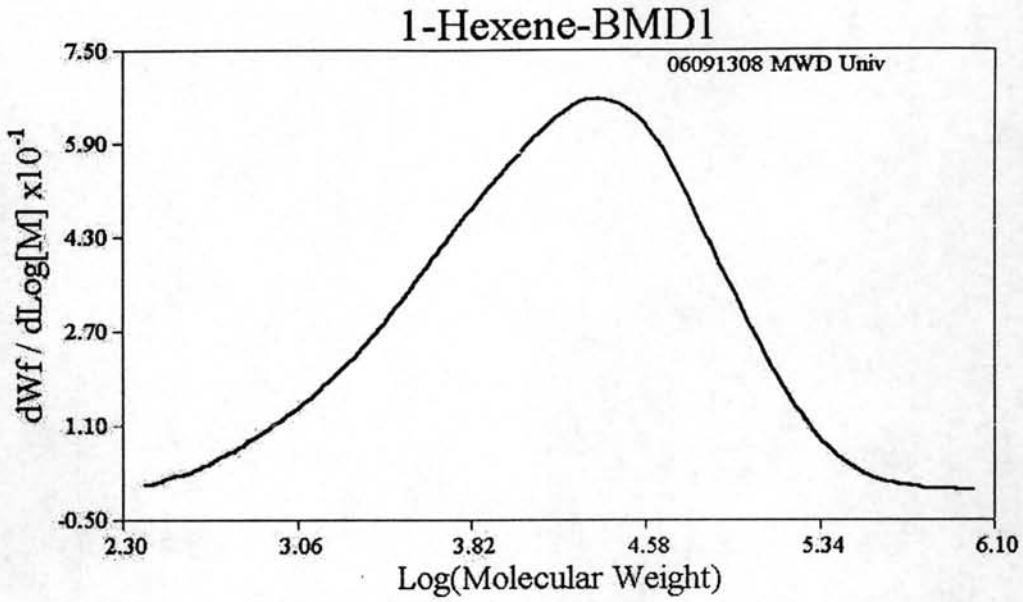


**Figure A-3** GPC curve of ethylene/1-hexene copolymer produce with MCM-41(BMD1)

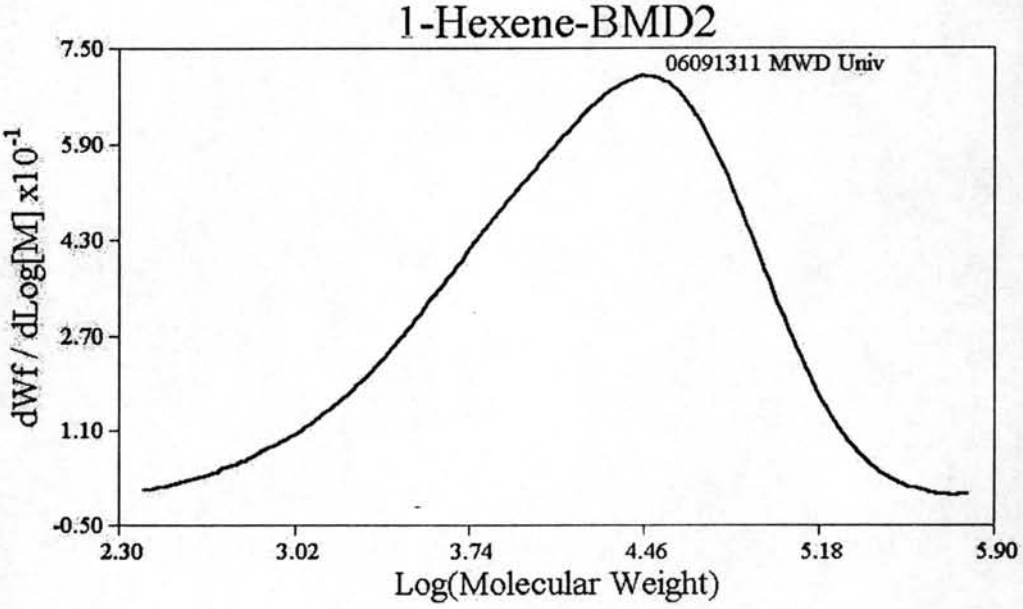


**Figure A-4** GPC curve of ethylene/1-hexene copolymer produce with MCM-41(BMD2)

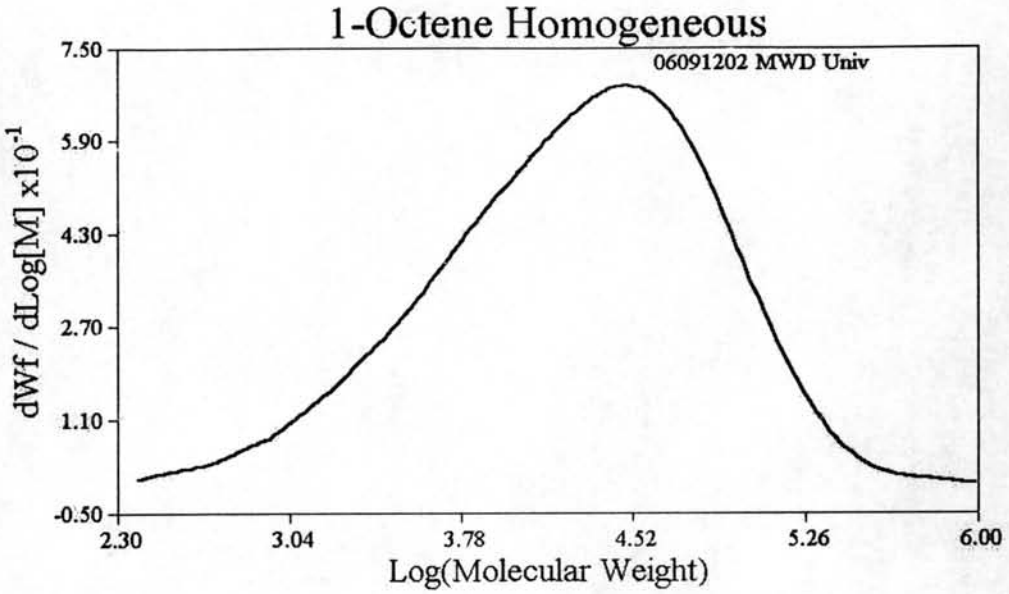


**Figure A-5** GPC curve of ethylene/1-octene copolymer produce with homogenous

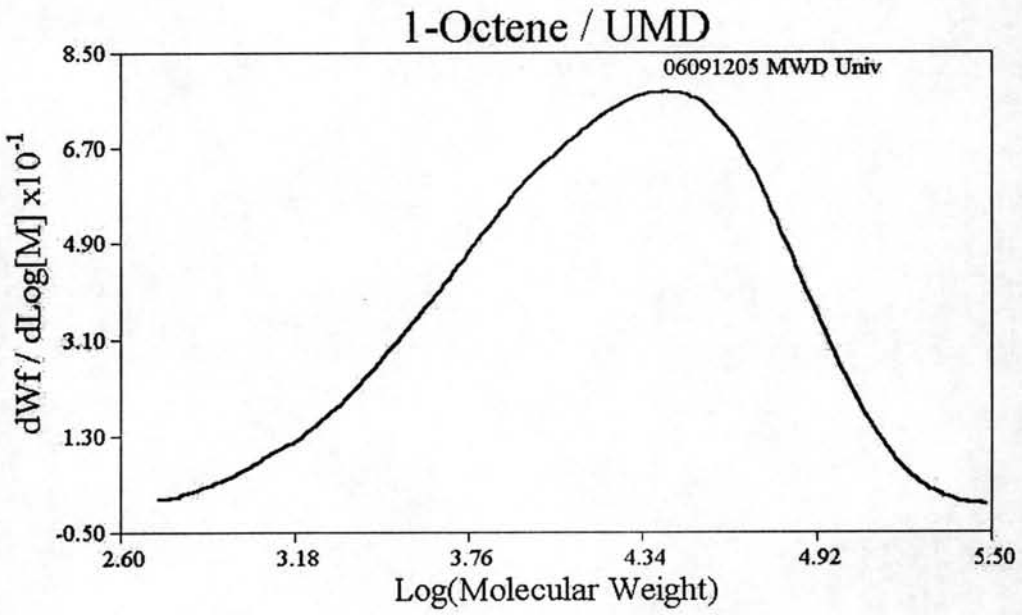


**Figure A-6** GPC curve of ethylene/1-octene copolymer produce with MCM-41(UMD)

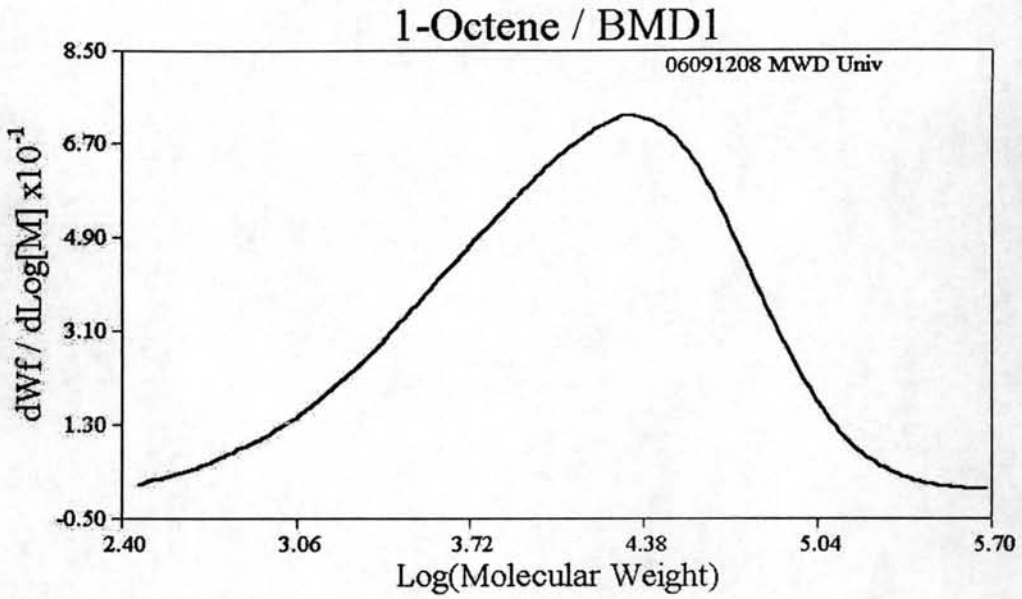


**Figure A-7** GPC curve of ethylene/1-octene copolymer produce with MCM-41(BMD1)

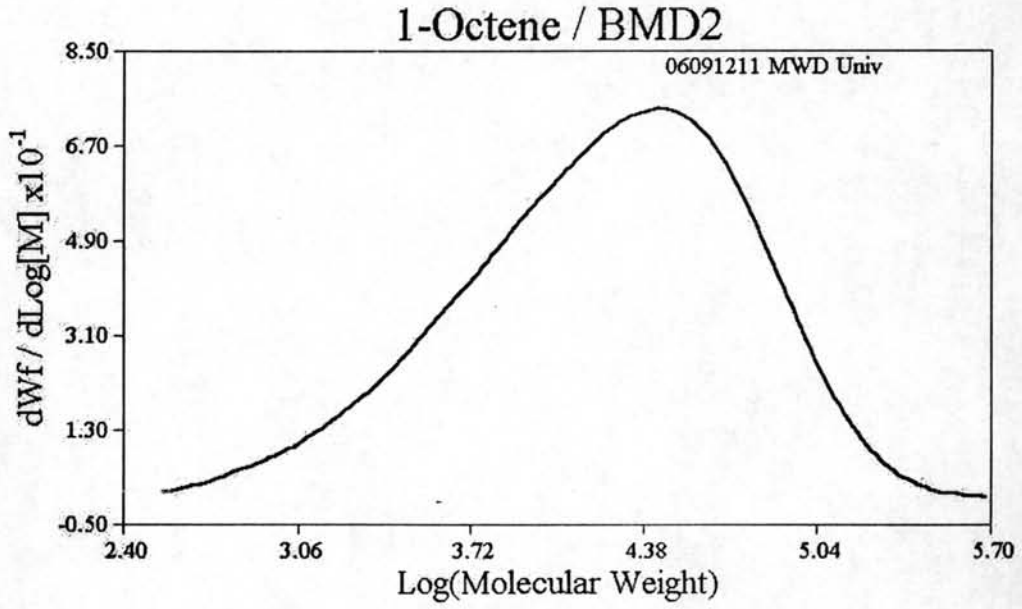


**Figure A-8** GPC curve of ethylene/1-octene copolymer produce with MCM-41(BMD2)

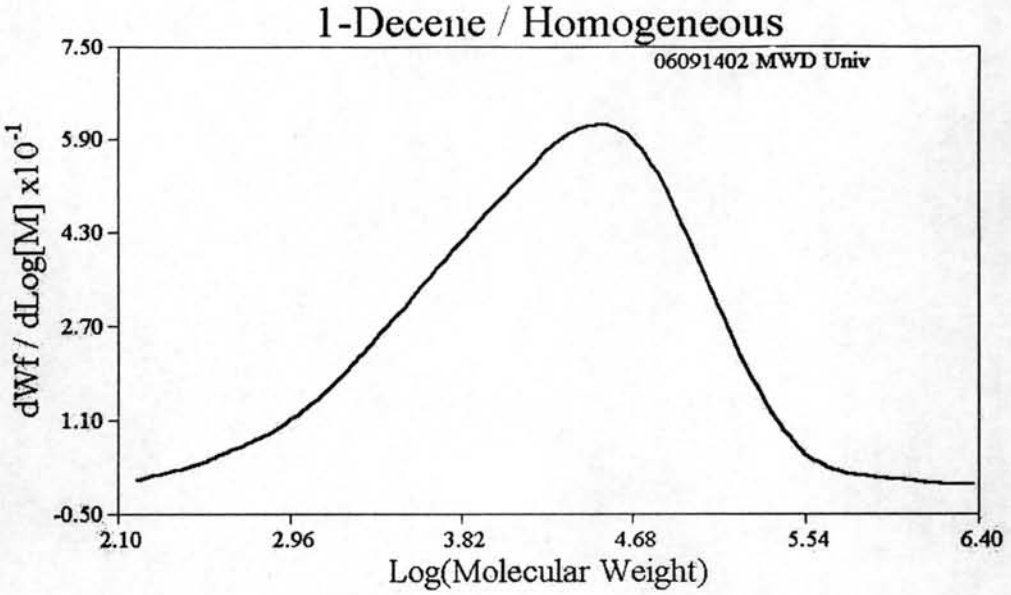


**Figure A-9** GPC curve of ethylene/1-decene copolymer produce with homogenous

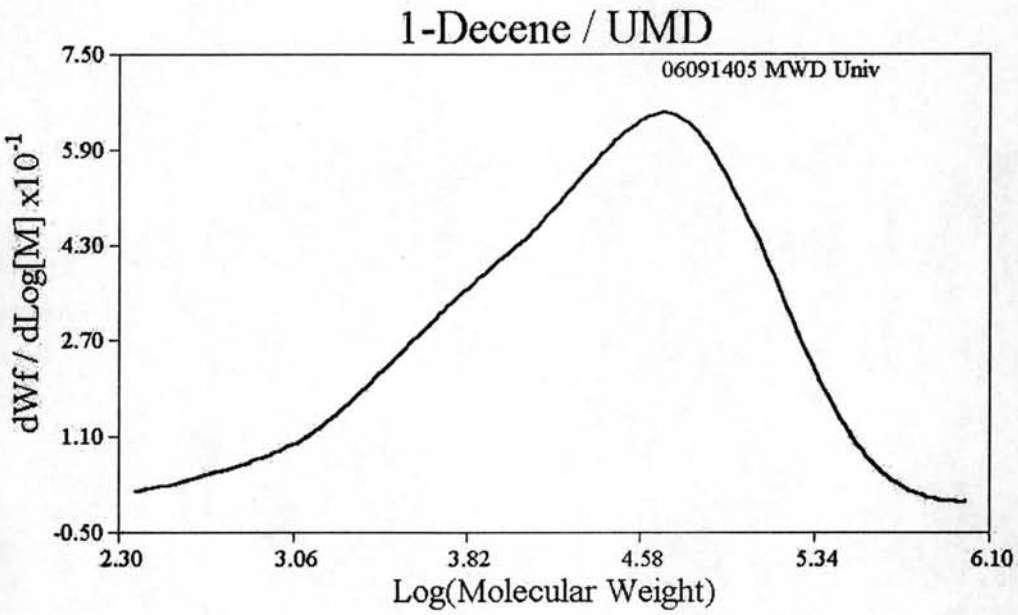


**Figure A-10** GPC curve of ethylene/1-decene copolymer produce with MCM-41(UMD)

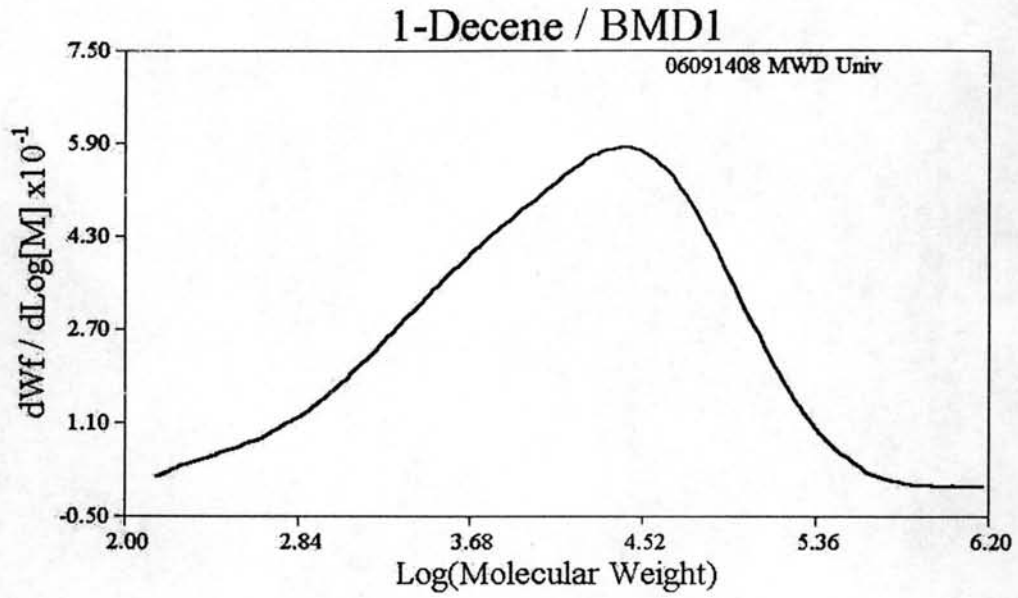


**Figure A-11** GPC curve of ethylene/1-decene copolymer produce with MCM-41(BMD1)

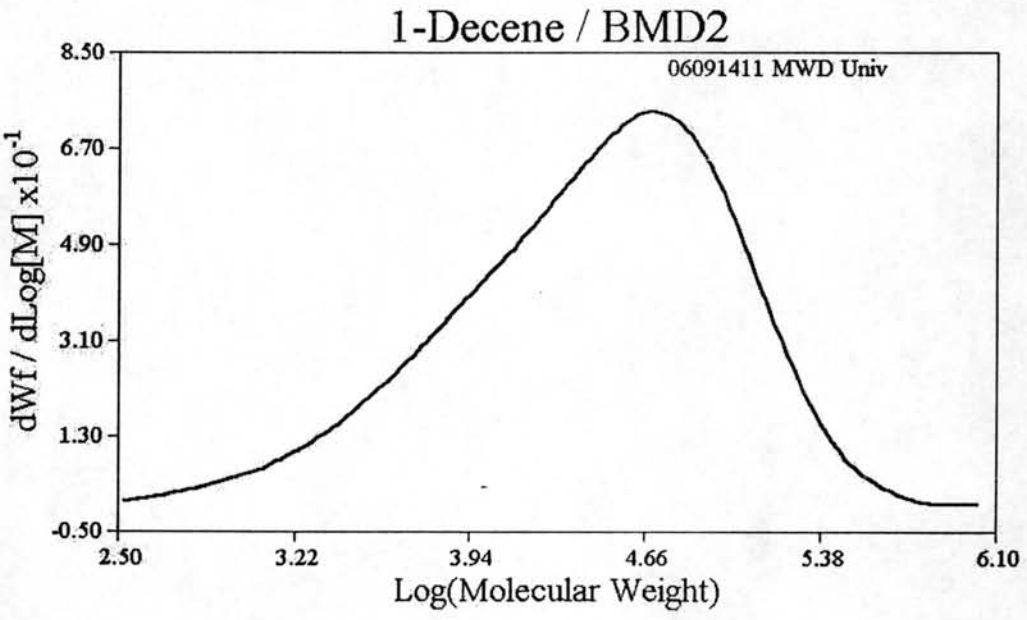


**Figure A-12** GPC curve of ethylene/1-decene copolymer produce with MCM-41(BMD2)

# APPENDIX B
# ( Differential scanning calorimeter)

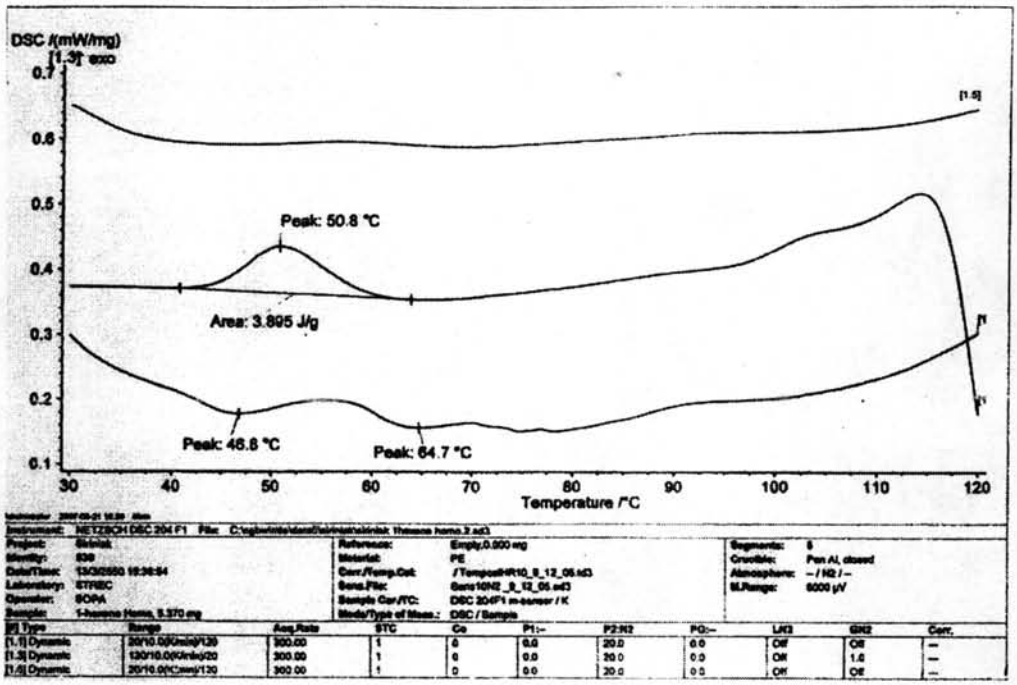


**Figure B-1** DSC curve of ethylene/1-hexene copolymer produce with homogenous

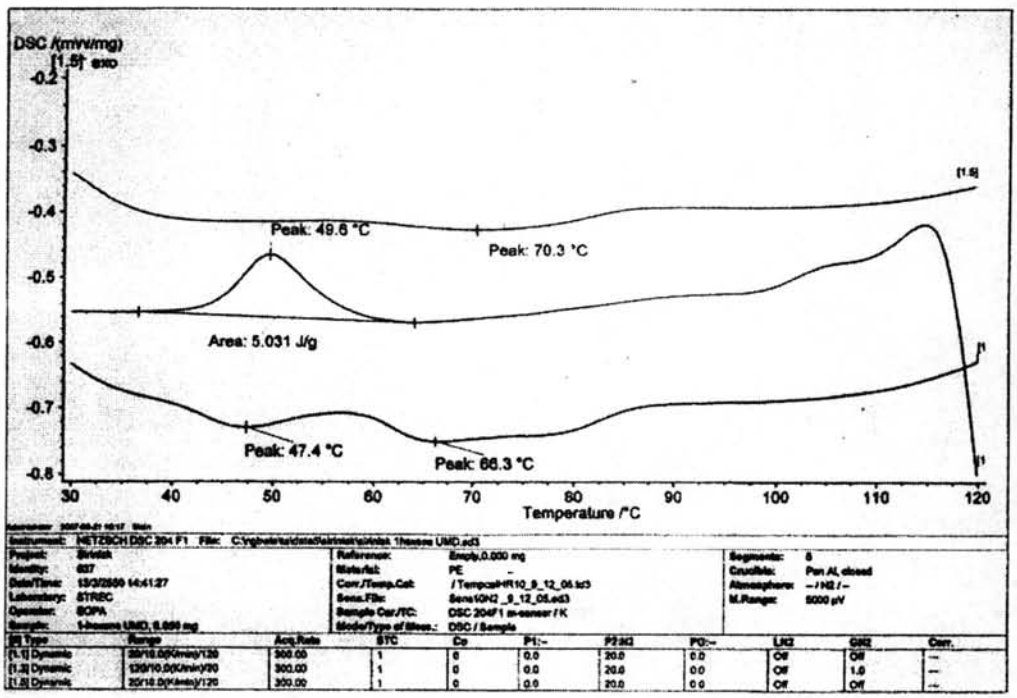


**Figure B-2** DSC curve of ethylene/1-hexene copolymer produce with MCM-41(UMD)

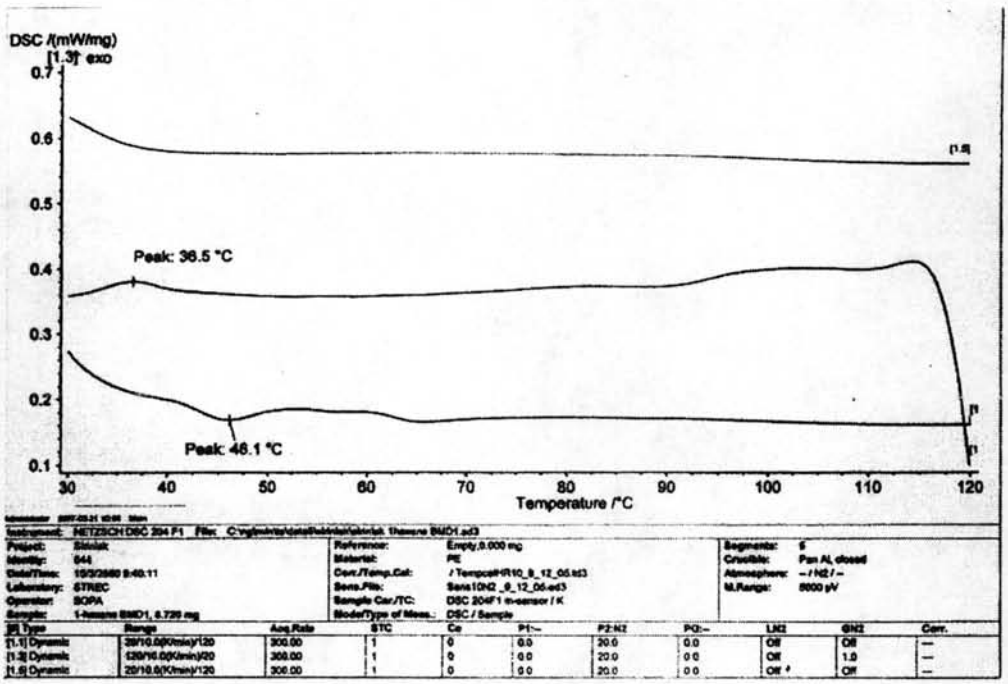


**Figure B-3** DSC curve of ethylene/1-hexene copolymer produce with MCM-41(BMD1)

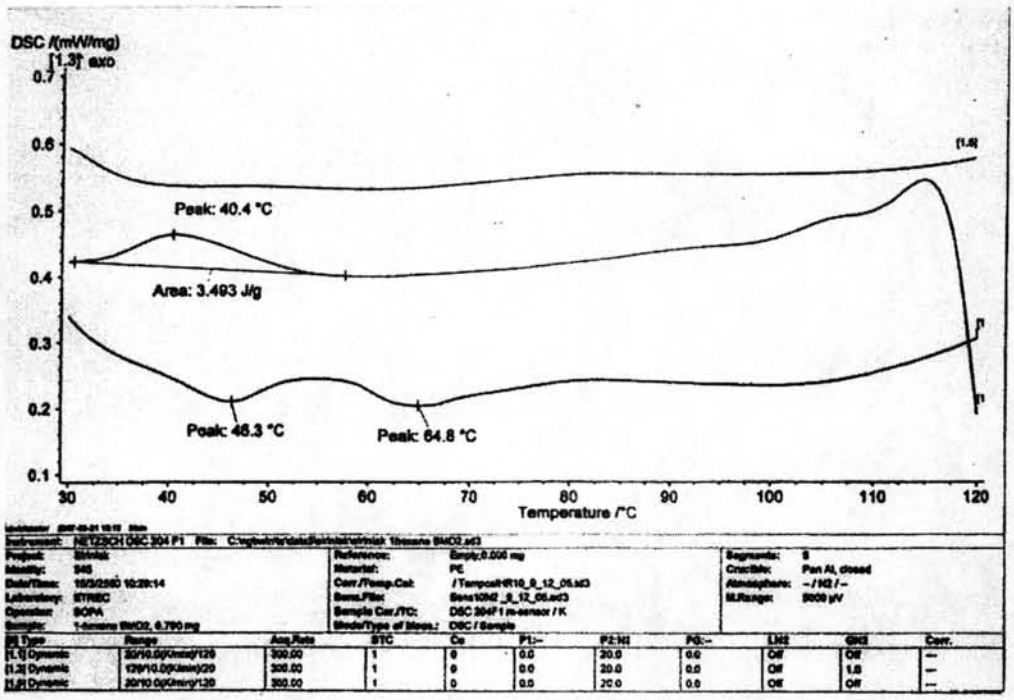


**Figure B-4** DSC curve of ethylene/1-hexene copolymer produce with MCM-41(BMD2)

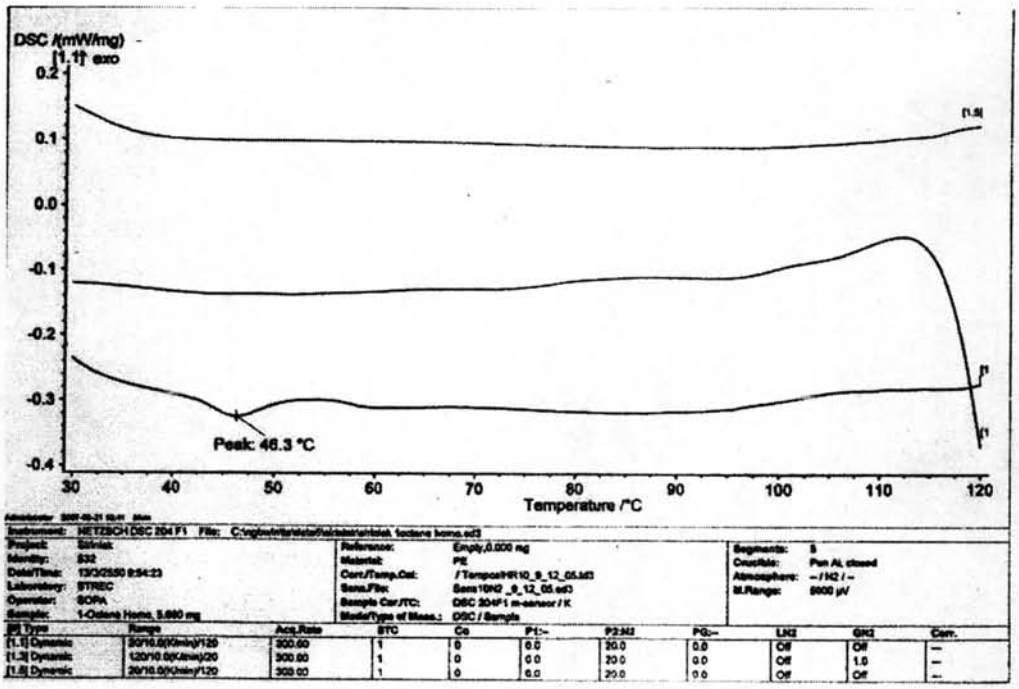


**Figure B-5** DSC curve of ethylene/1-octene copolymer produce with homogenous

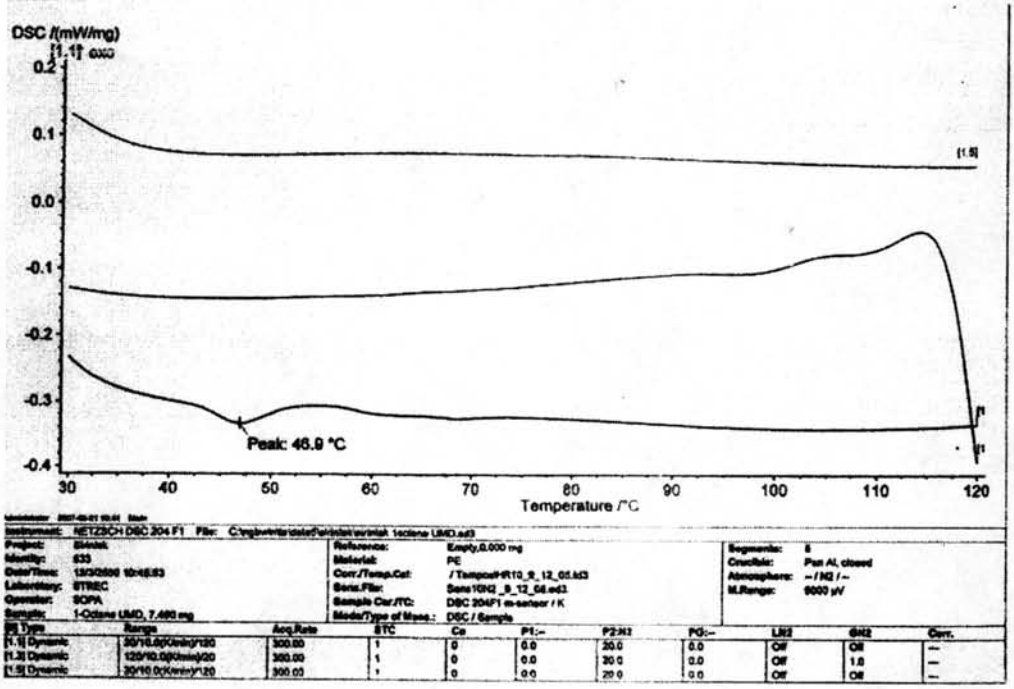


**Figure B-6** DSC curve of ethylene/1-octene copolymer produce with MCM-41(UMD)

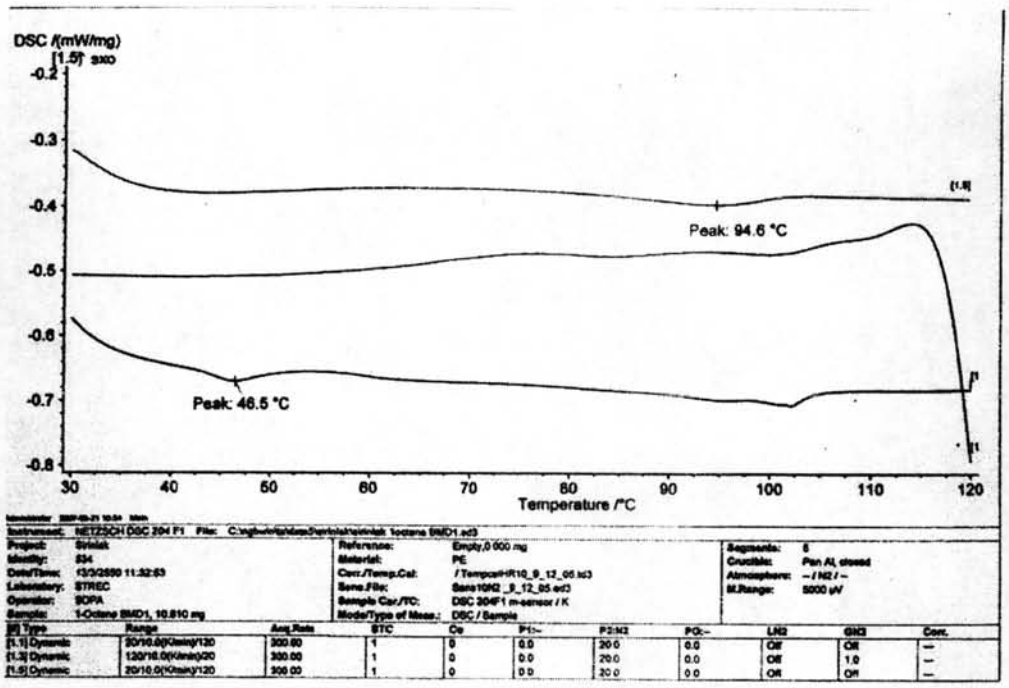


**Figure B-7** DSC curve of ethylene/1-octene copolymer produce with MCM-41(BMD1)

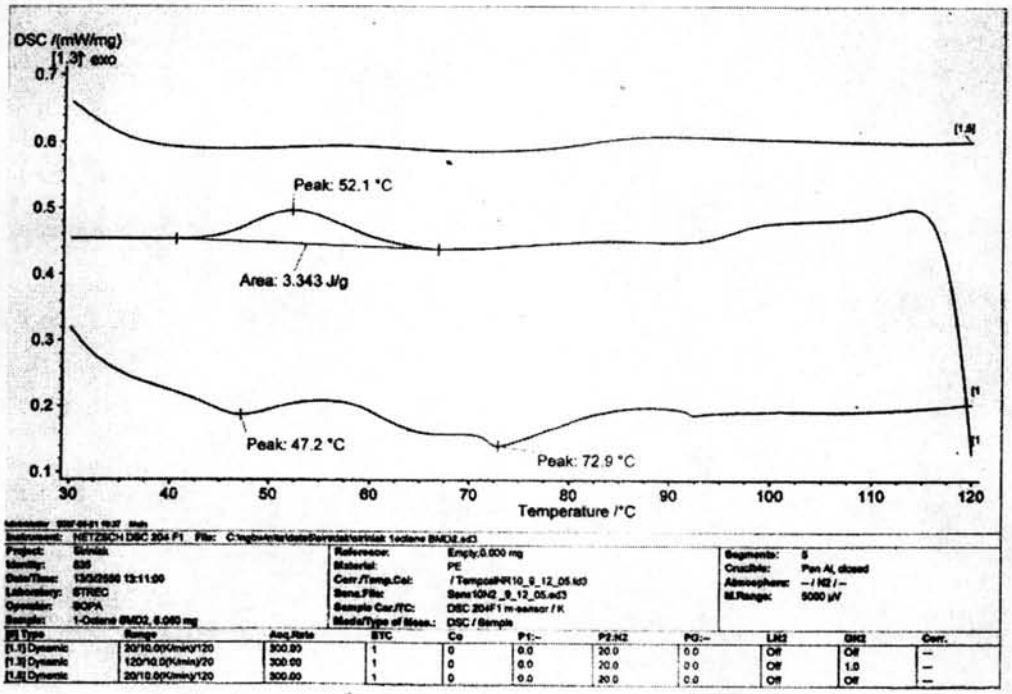


**Figure B-8** DSC curve of ethylene/1-octene copolymer produce with MCM-41(BMD2)

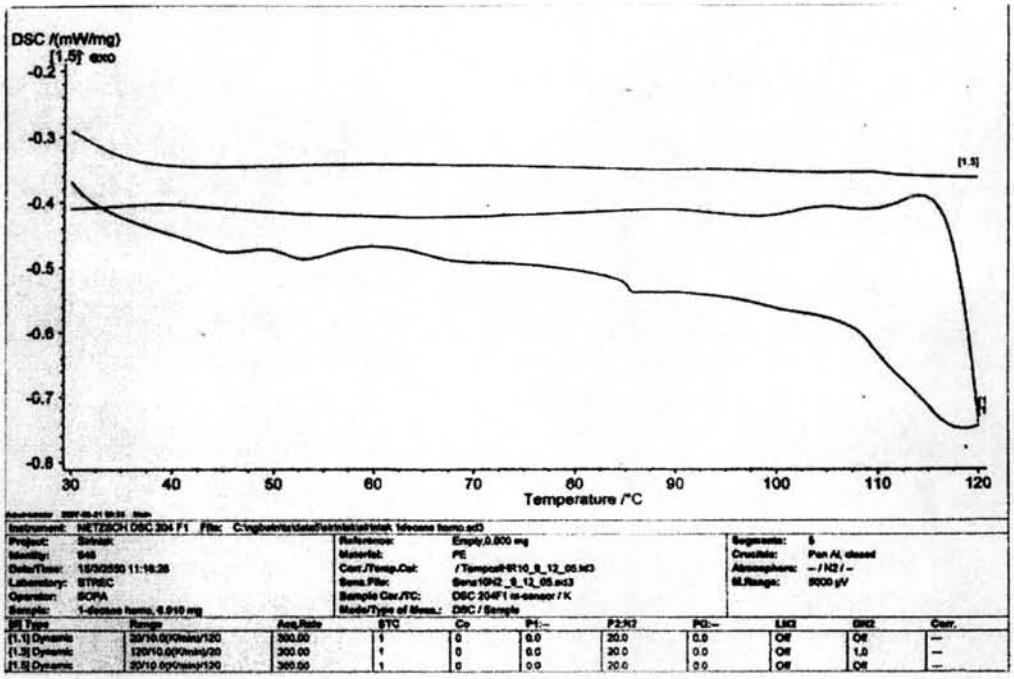


**Figure B-9** DSC curve of ethylene/1-decene copolymer produce with homogenous

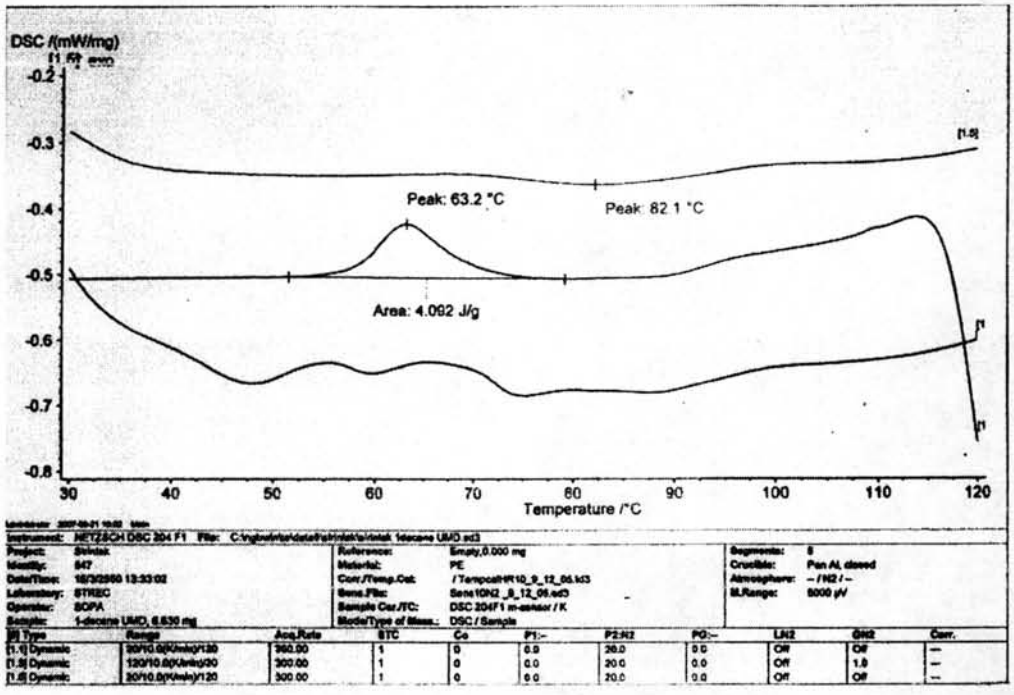


**Figure B-10** DSC curve of ethylene/1-decene copolymer produce with MCM-41(UMD)

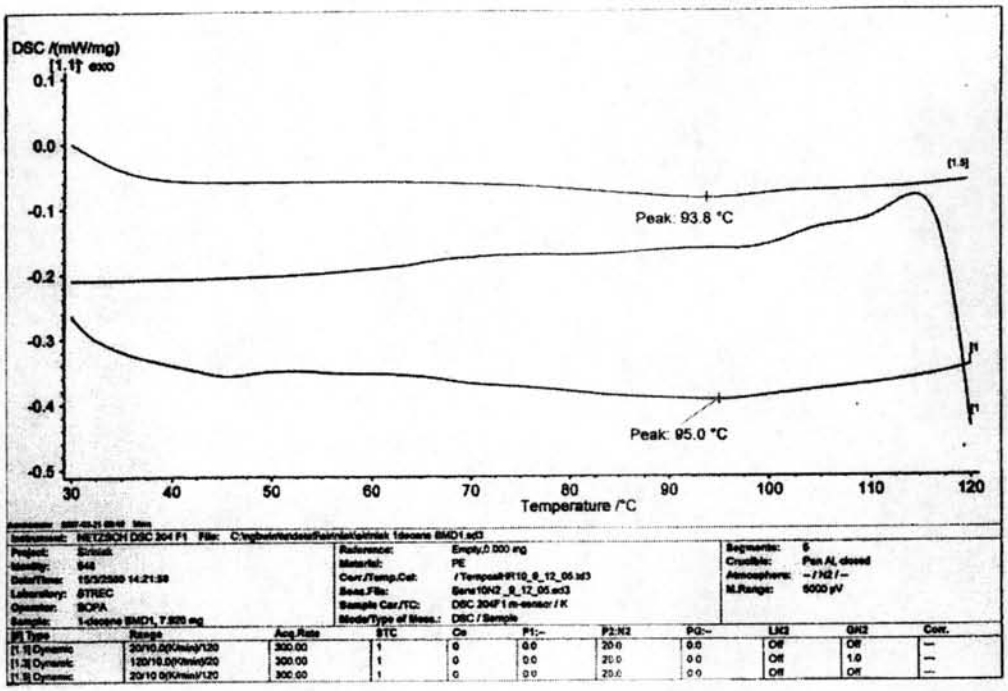


**Figure B-11** DSC curve of ethylene/1-decene copolymer produce with MCM-41(BMD1)

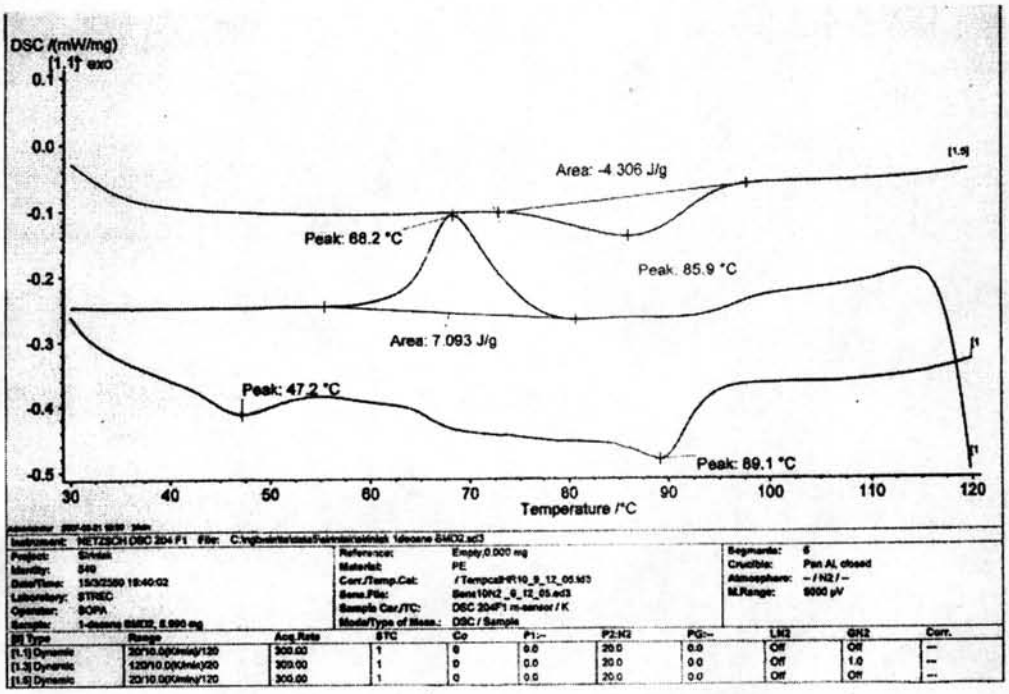


**Figure B-12** DSC curve of ethylene/1-decene copolymer produce with MCM-41(BMD)

# APPENDIX C
# ( Nuclear magnetic resonance )

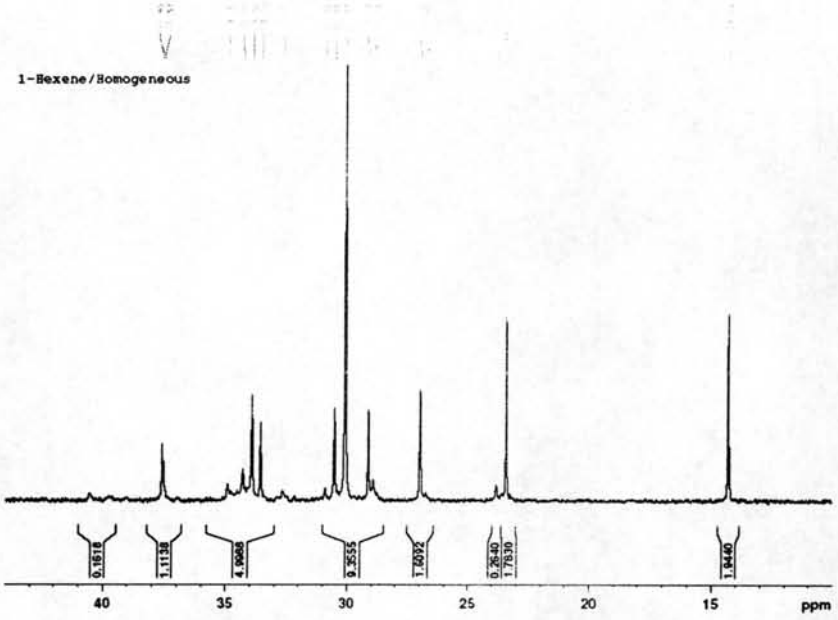


**Figure C-1** $^{13}$C-NMR spectrum of ethylene/1-hexene copolymer produce with homogenous

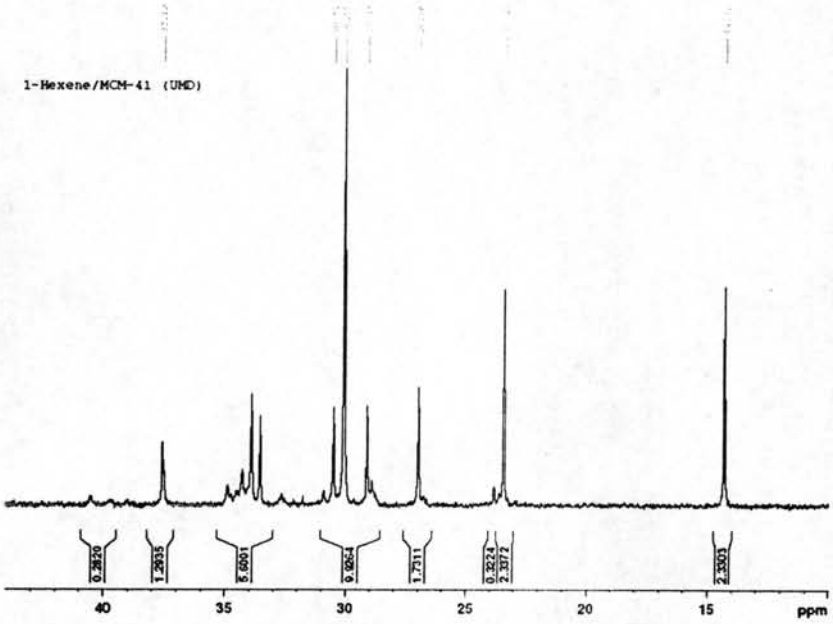


**FigureC-2** $^{13}$C-NMR spectrum of ethylene/1-hexene copolymer produce with MCM-41(UMD)

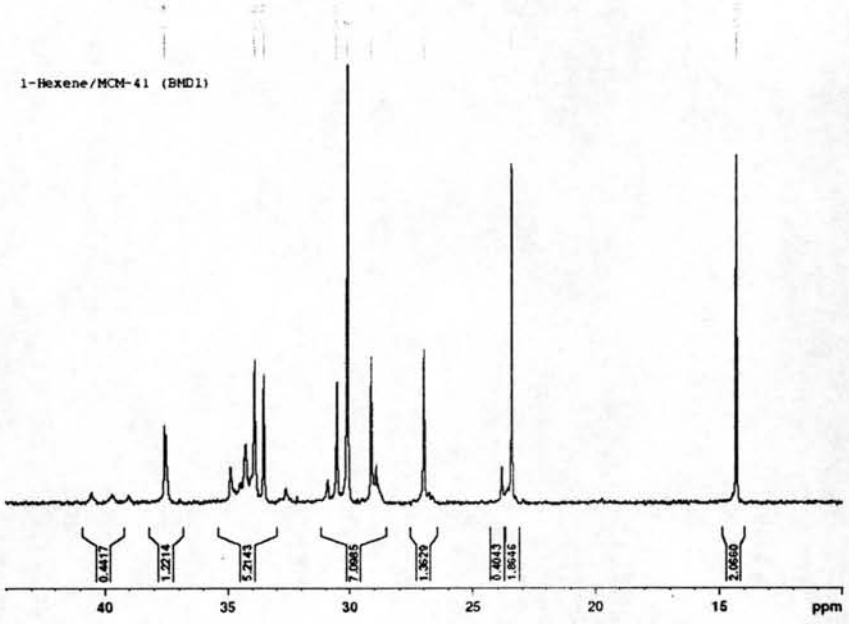


**Figure C-3** $^{13}$C-NMR spectrum of ethylene/1-hexene copolymer produce with MCM-41(BMD1)

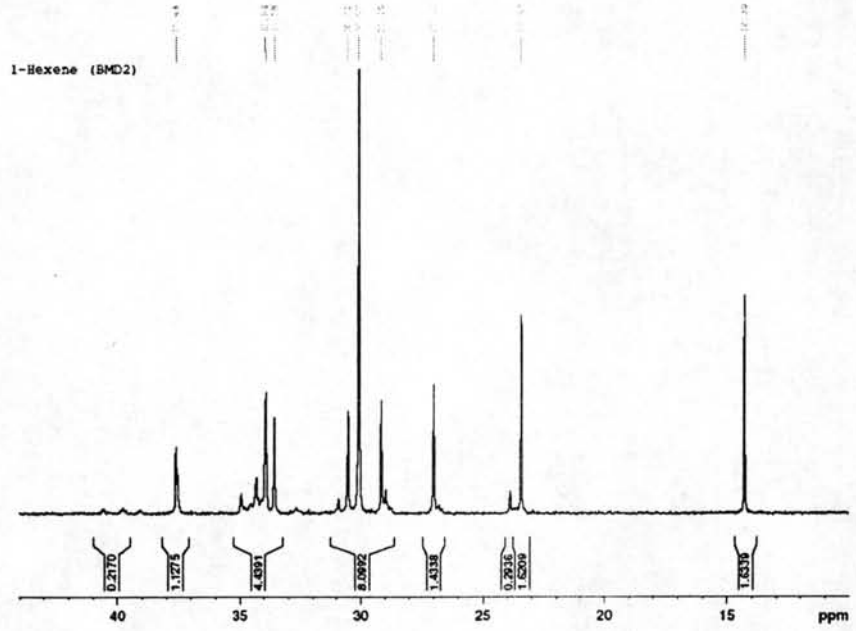


**Figure C-4** $^{13}$C-NMR spectrum of ethylene/1-hexene copolymer produce with MCM-41(BMD2)

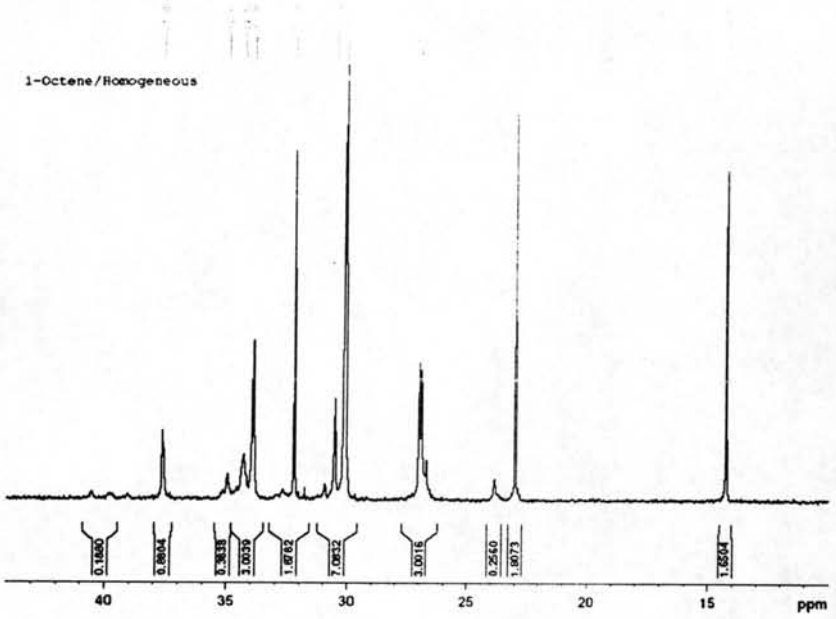


**Figure C-5** $^{13}$C-NMR spectrum of ethylene/1-octene copolymer produce with homogenous

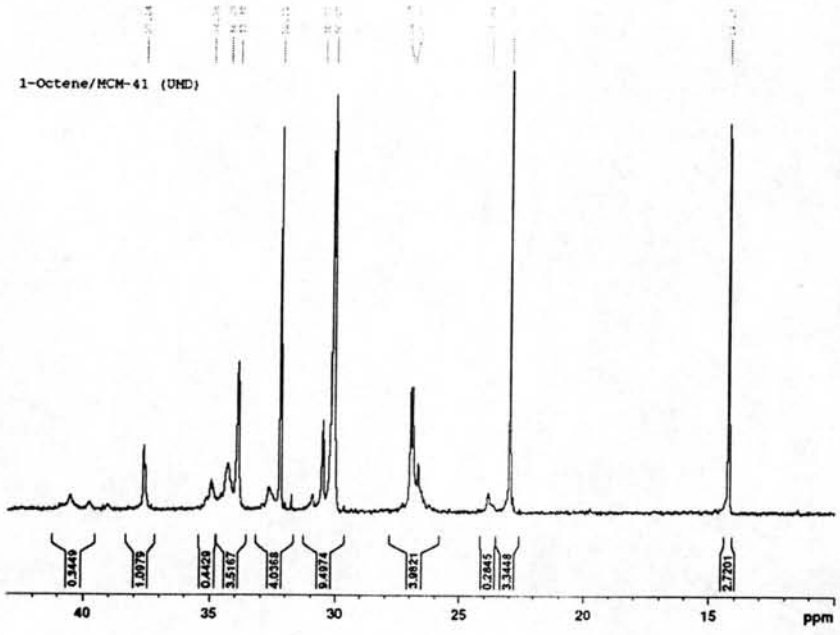


**Figure C-6** $^{13}$C-NMR spectrum of ethylene/1-octene copolymer produce with MCM-41(UMD)

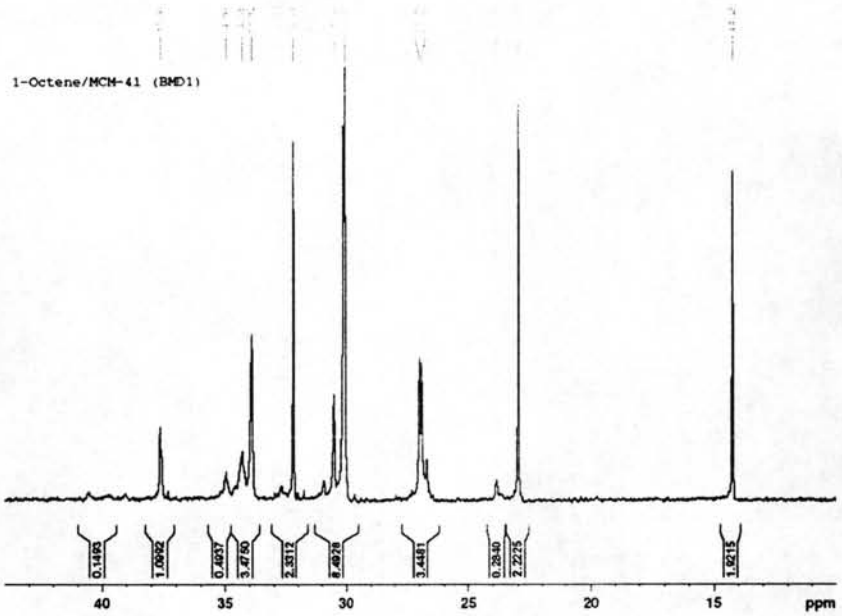


**Figure C-7** $^{13}$C-NMR spectrum of etylene/1-octene copolymer produce with MCM-41(BMD1)

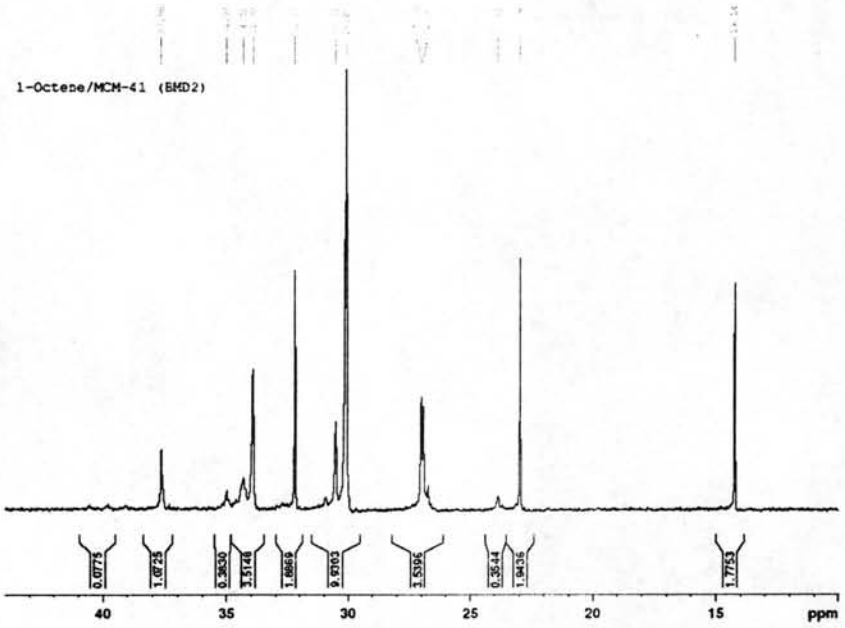


**Figure C-8** $^{13}$C-NMR spectrum of ethylene/1-octene copolymer produce with MCM-41(BMD2)

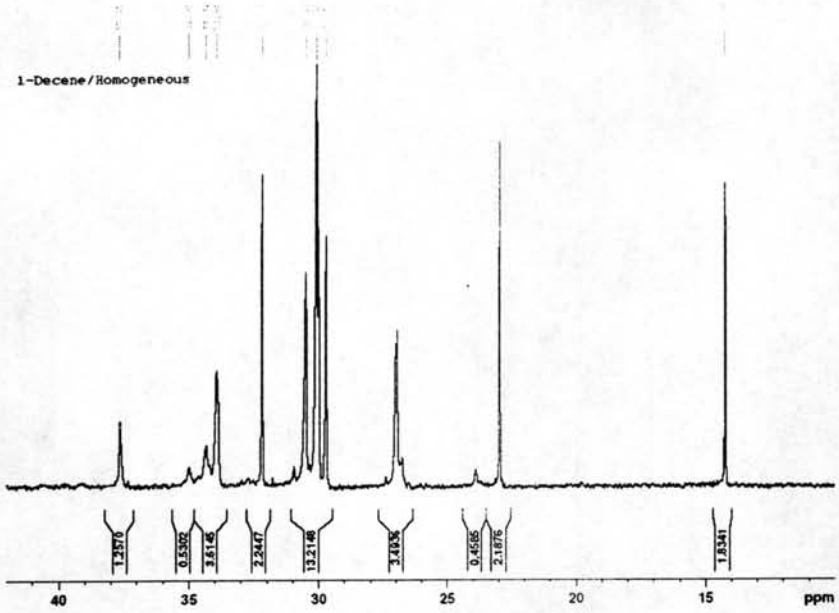


**Figure C-9** $^{13}$C-NMR spectrum of ethylene/1-decene copolymer produce with homogenous

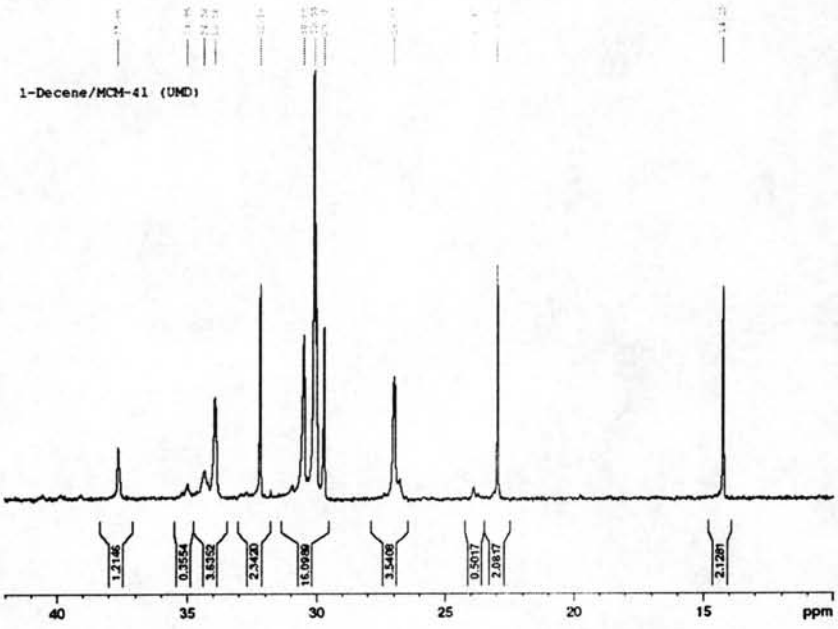


**Figure C-10** $^{13}$C-NMR spectrum of ethylene/1-decene copolymer produce with MCM-41(UMD)

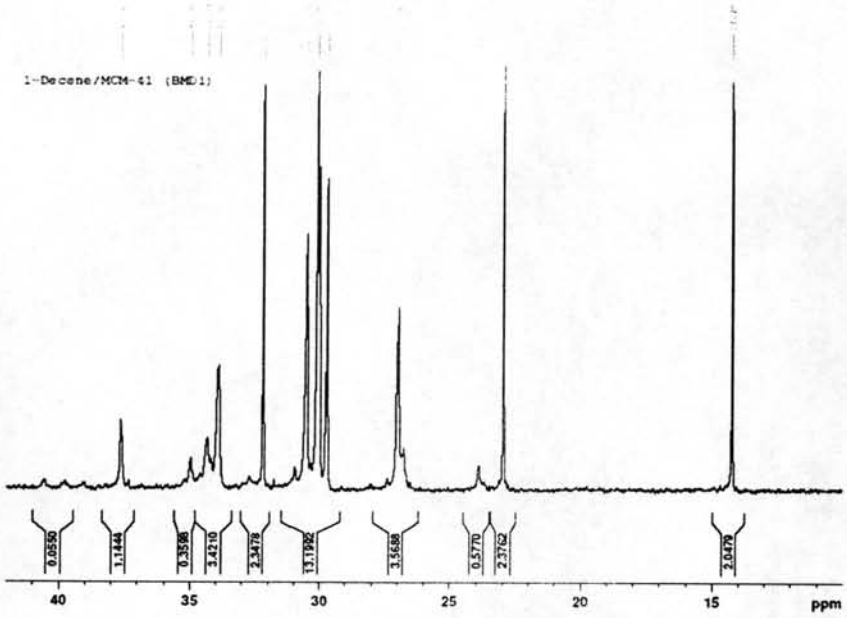


**Figure C-11** $^{13}$C-NMR spectrum of ethylene/1-decene copolymer produce with MCM-41(BMD1)

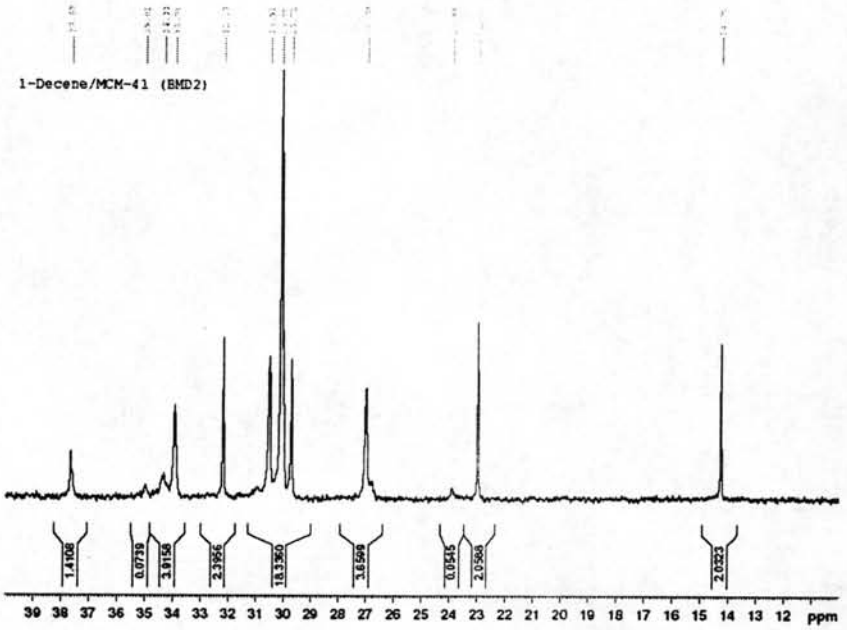


**Figure C-12** $^{13}$C-NMR spectrum of ethylene/1-decene copolymer produce with MCM-41(BMD2)

# APPENDIX D
# ( Thermogravimetric analysis )

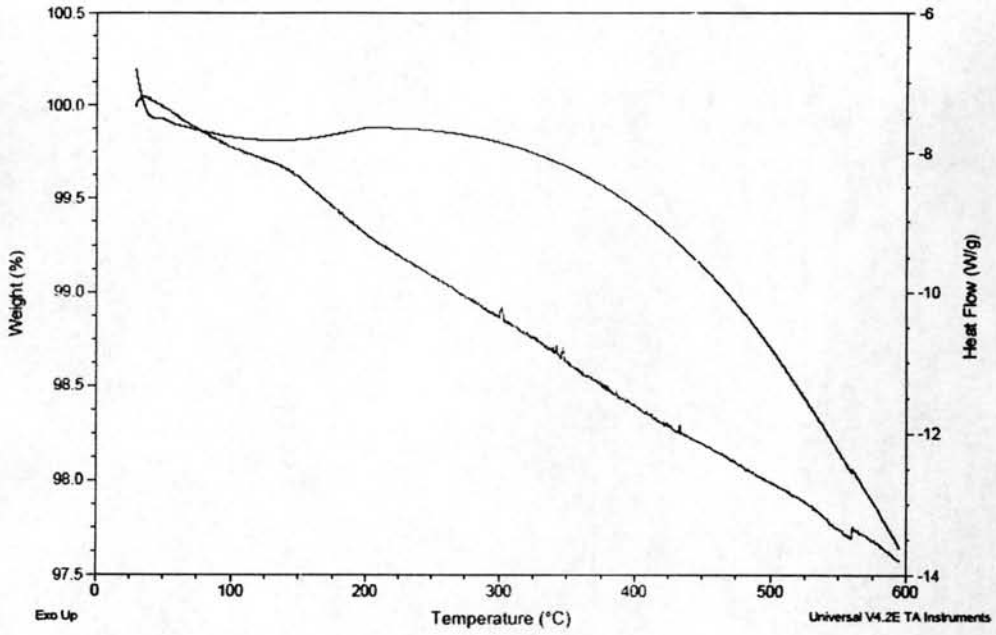


**Figure D-1** The TGA profiles MCM-41(UMD) supports

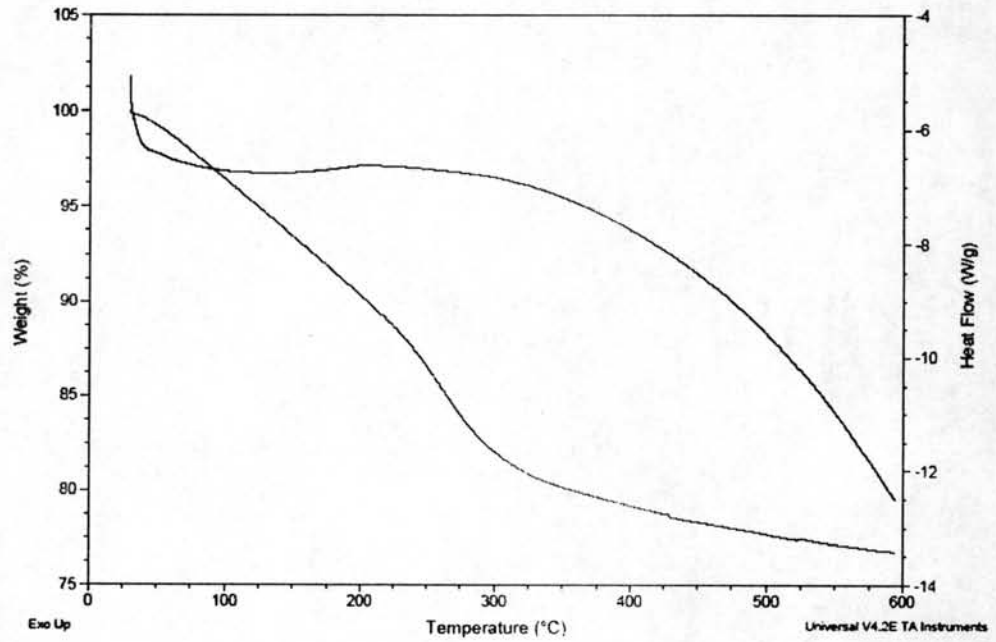


**Figure D-2** The TGA profiles MCM-41(BMD1) supports

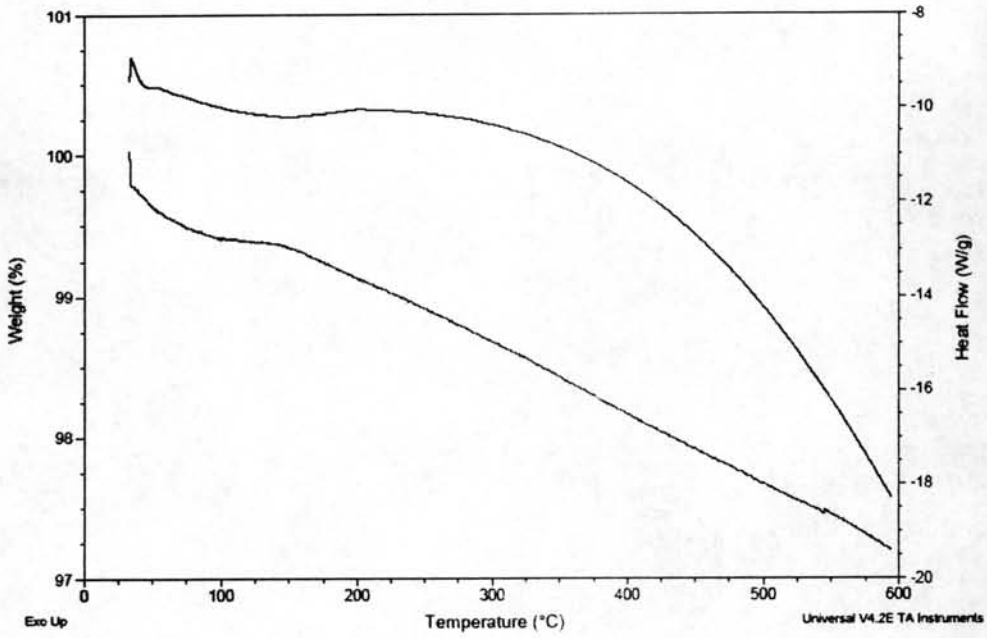


**Figure D-3** The TGA profiles MCM-41(BMD2) supports

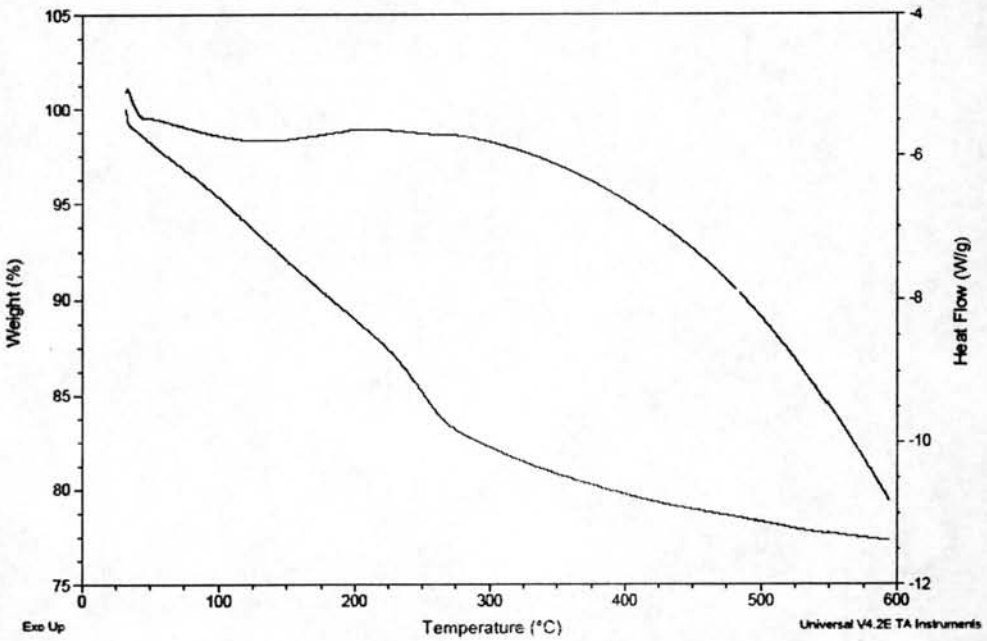


**Figure D-4** The TGA profiles of $[Al]_{dMMAO}$ on MCM-41(UMD) supports

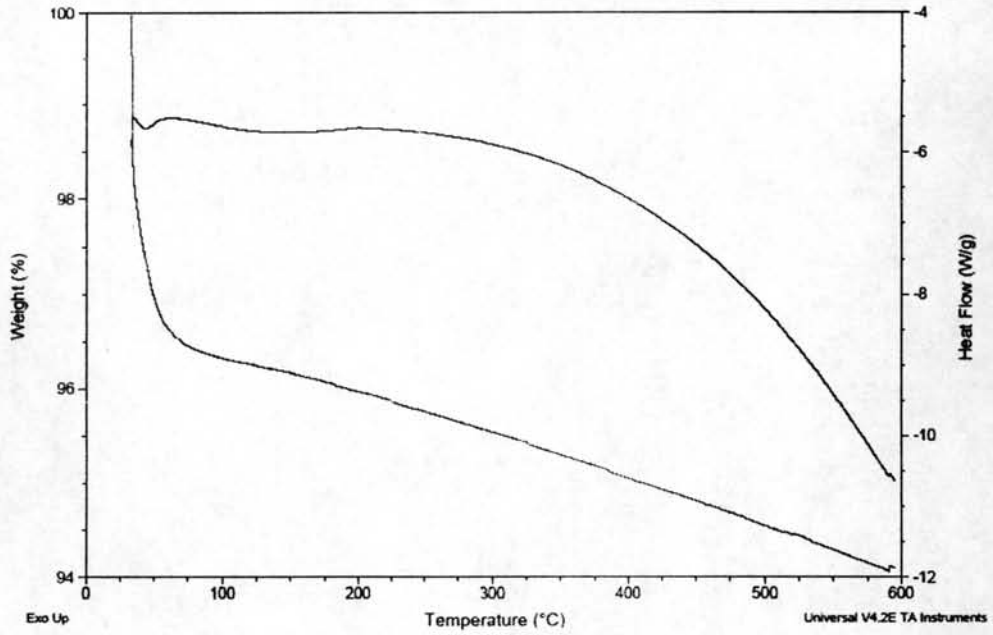


**Figure D-5** The TGA profiles of $[Al]_{dMMAO}$ on MCM-41(BMD1) supports

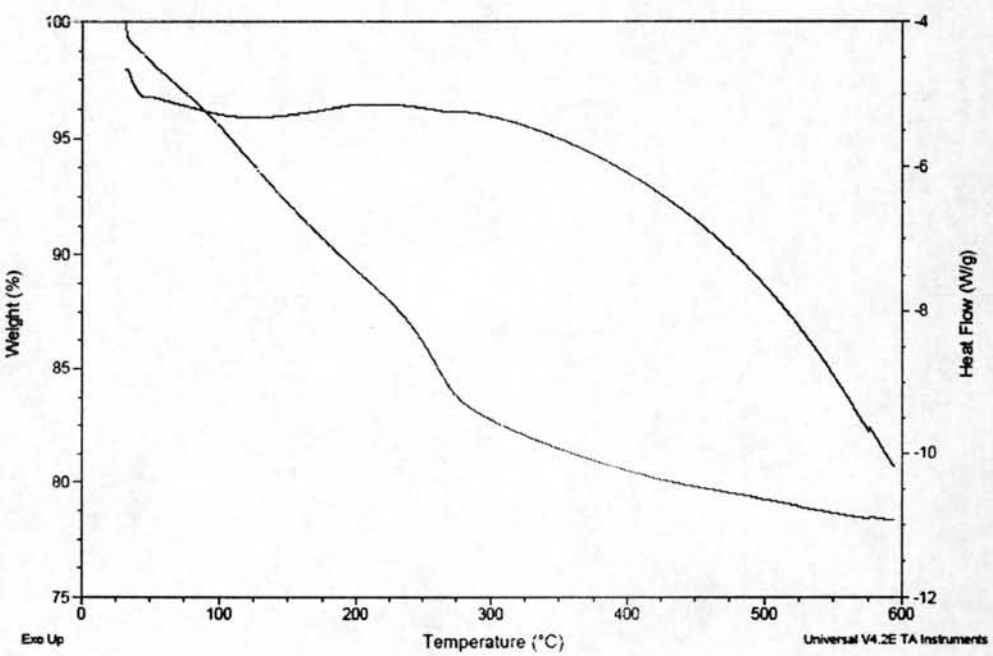


**Figure D-6** The TGA profiles of $[Al]_{dMMAO}$ on MCM-41(BMD2) supports

# APPENDIX E
(X-ray photoelectron spectroscopy)

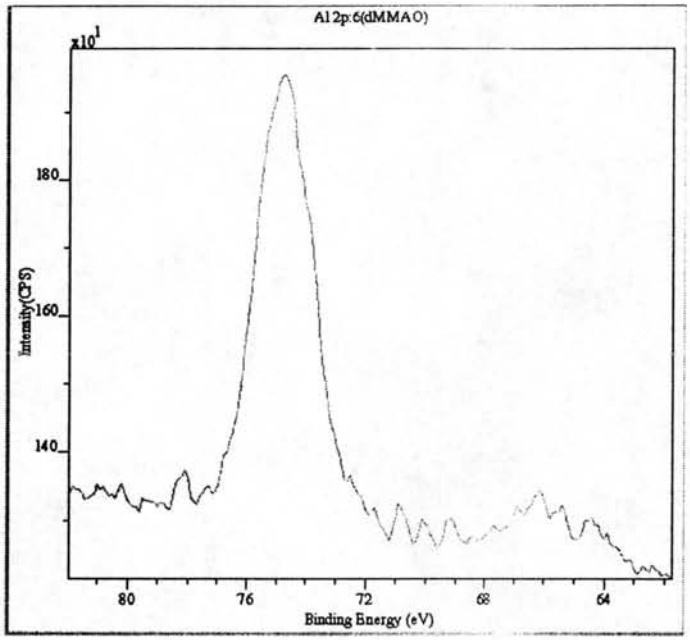


**Figure E-1** The typical XPS profile for dMMAO exhibited the identical binding energy (BE) of Al 2p

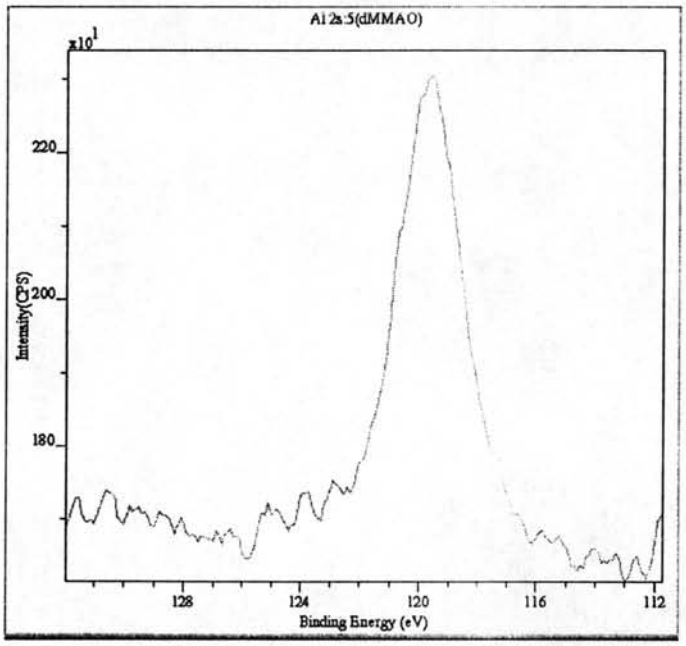


**Figure E-2** The typical XPS profile for dMMAO exhibited the identical binding energy (BE) of Al 2s

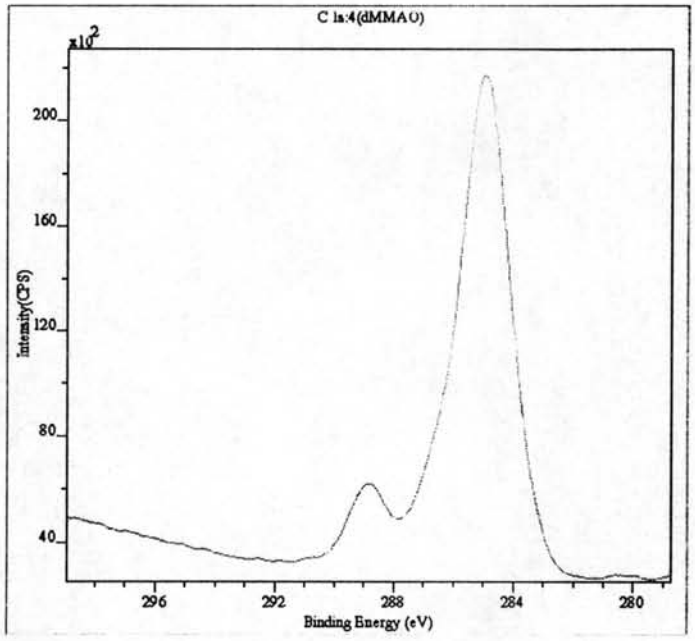


**Figure E-3** The typical XPS profile for dMMAO exhibited the identical binding energy (BE) of C 1s

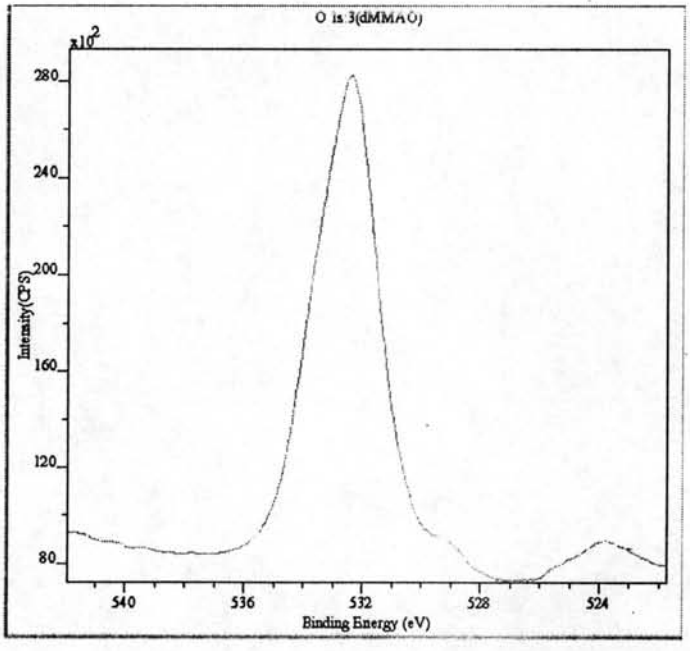


**Figure E-4** The typical XPS profile for dMMAO exhibited the identical binding energy (BE) of O 1s

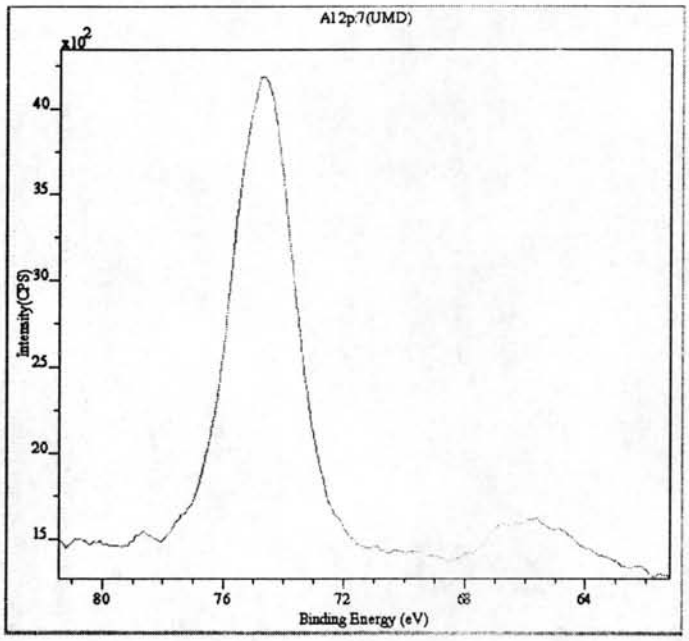


**Figure E-5** The typical XPS profile for MCM-41(UMD)-supported dMMAO exhibited the identical binding energy (BE) of Al 2p

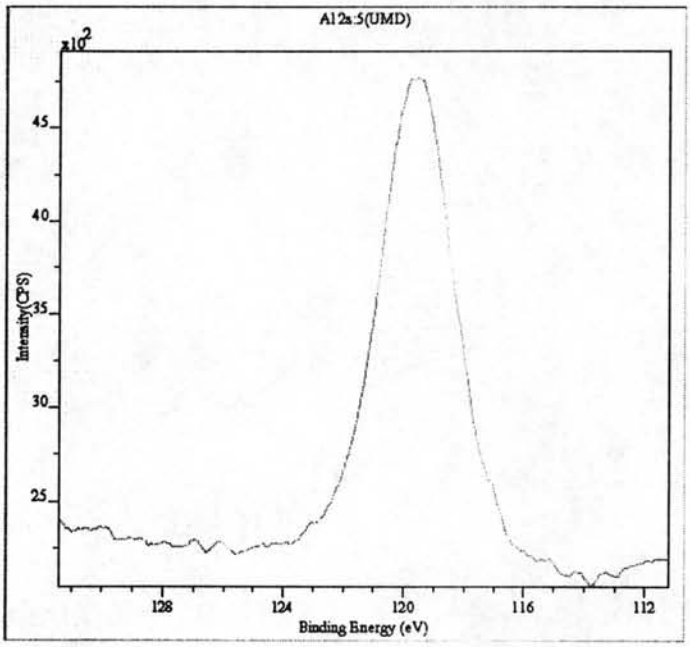


**Figure E-6** The typical XPS profile for MCM-41(UMD)-supported dMMAO exhibited the identical binding energy (BE) of Al 2s

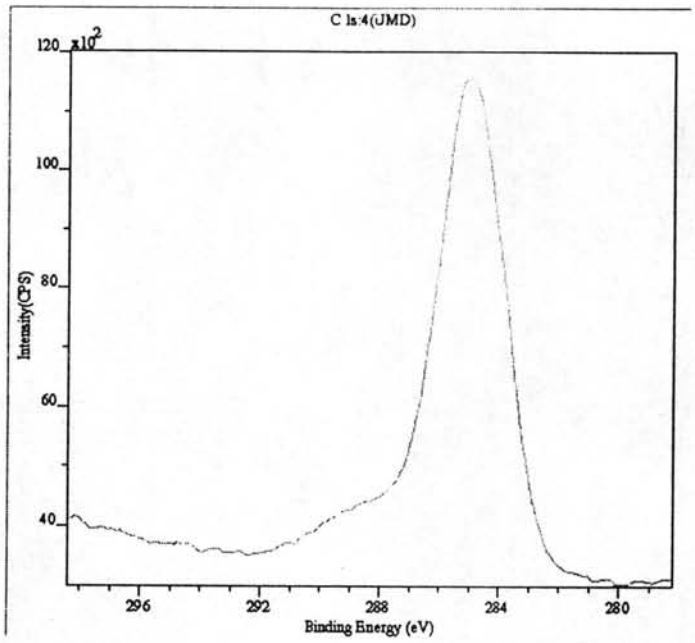


**Figure E-7** The typical XPS profile for MCM-41(UMD)-supported dMMAO exhibited the identical binding energy (BE) of C 1s

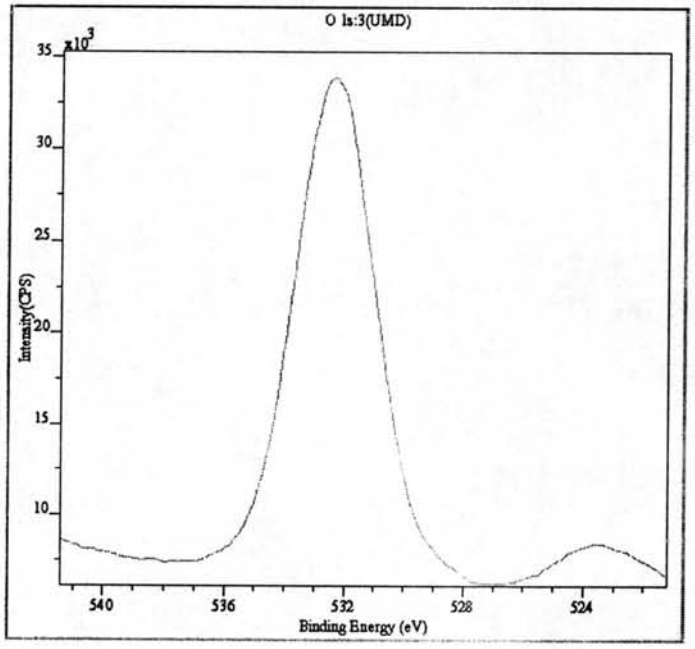


**Figure E-8** The typical XPS profile for MCM-41(UMD)-supported dMMAO exhibited the identical binding energy (BE) of O 1s

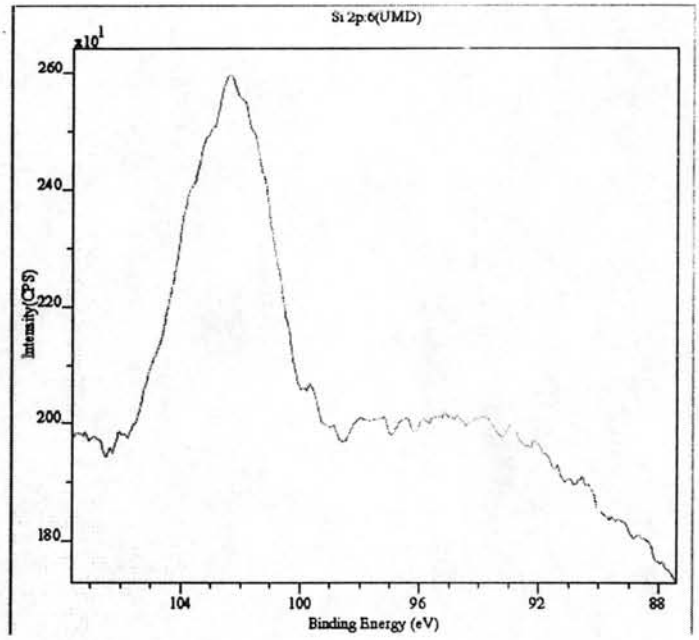


**Figure E-9** The typical XPS profile for MCM-41(UMD)-supported dMMAO exhibited the identical binding energy (BE) of Si 2p

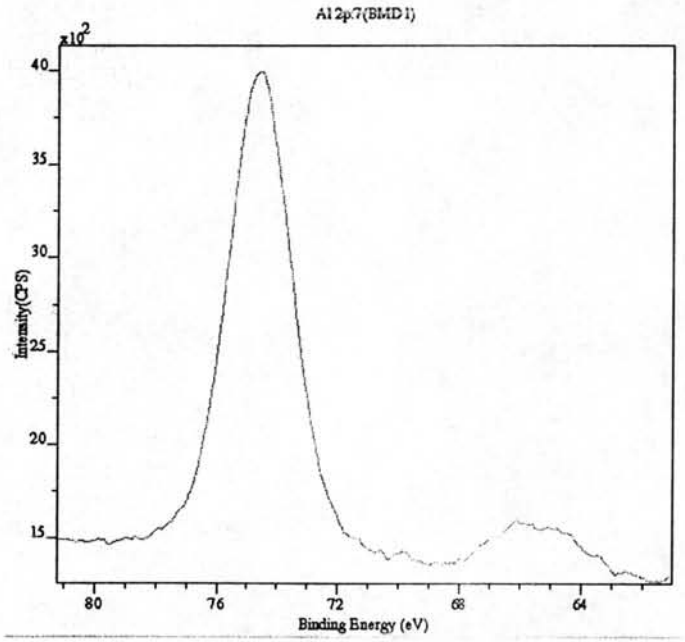


**Figure E-10** The typical XPS profile for MCM-41(BMD1)-supported dMMAO exhibited the identical binding energy (BE) of Al 2p

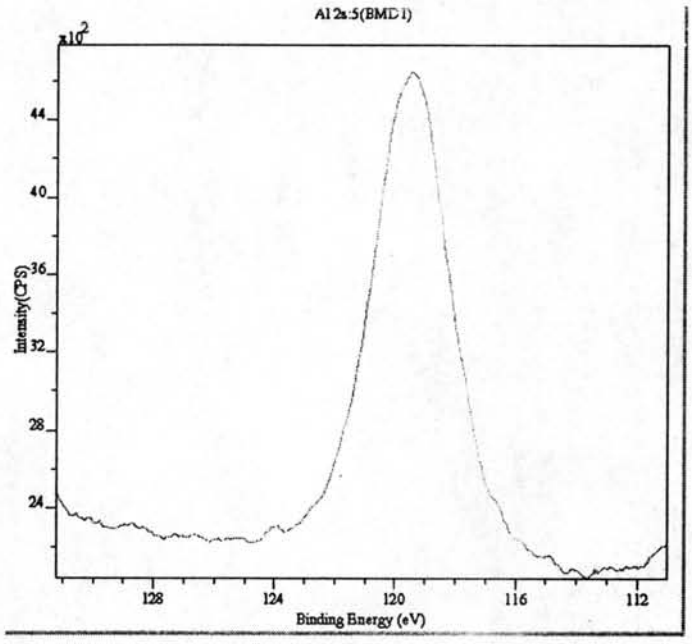


**Figure E-11** The typical XPS profile for MCM-41(BMD1)-supported dMMAO exhibited the identical binding energy (BE) of Al 2s

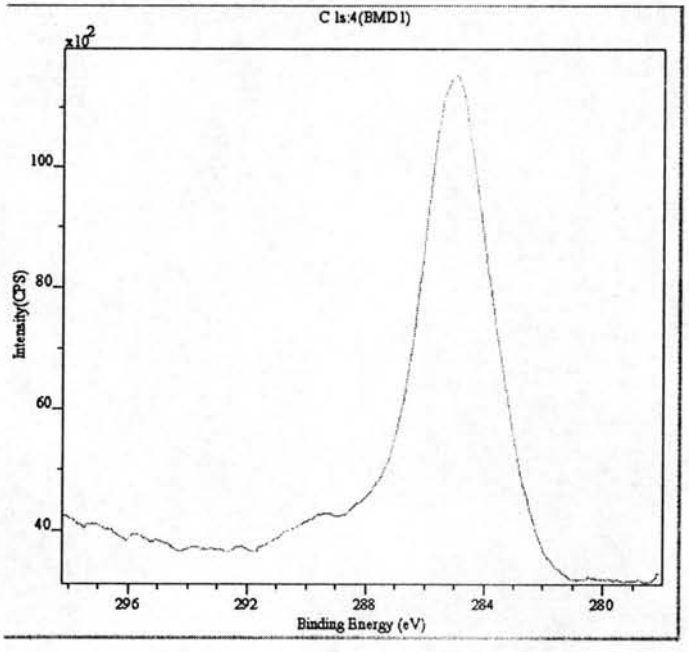


**Figure E-12** The typical XPS profile for MCM-41(BMD1)-supported dMMAO exhibited the identical binding energy (BE) of C 1s

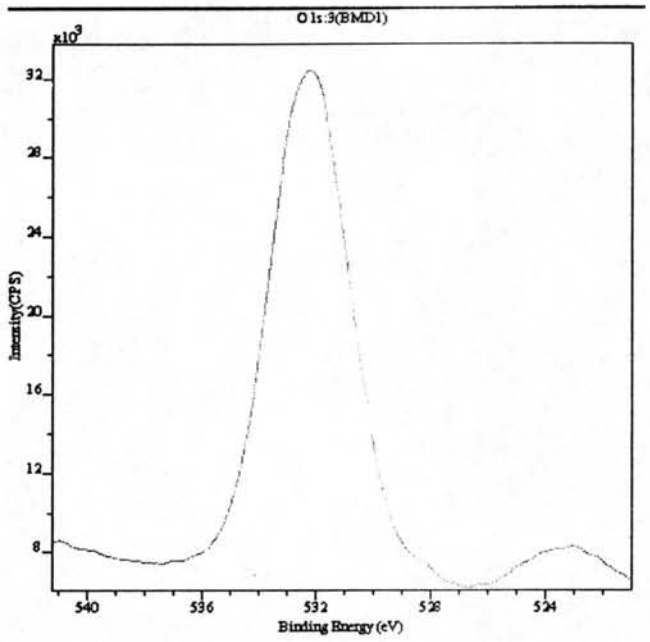


**Figure E-13** The typical XPS profile for MCM-41(BMD1)-supported dMMAO exhibited the identical binding energy (BE) of O 1s

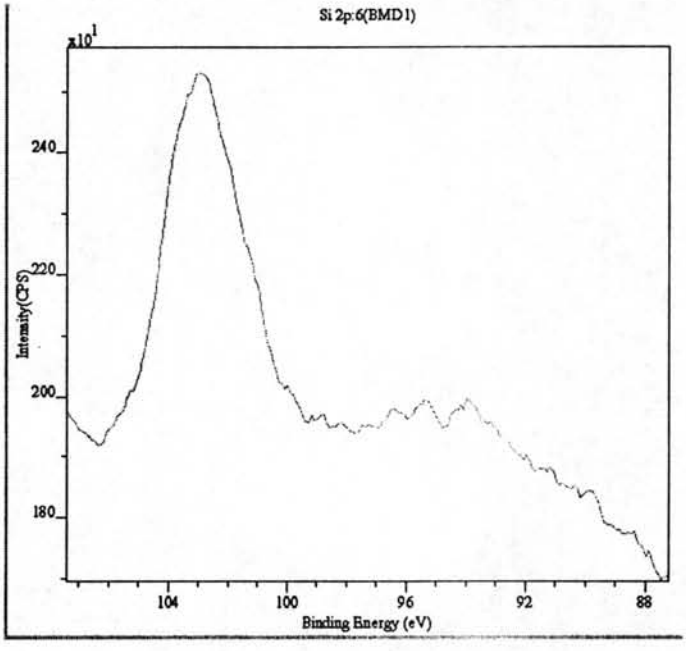


**Figure E-14** The typical XPS profile for MCM-41(BMD1)-supported dMMAO exhibited the identical binding energy (BE) of Si 2p

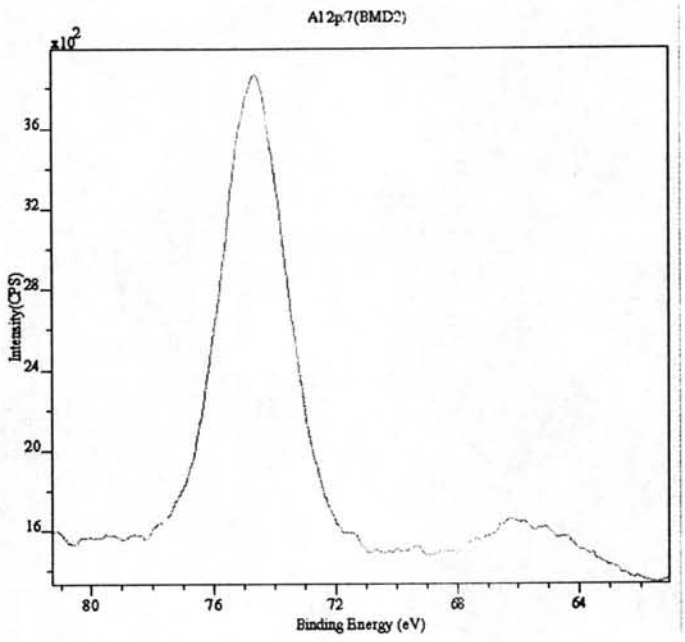


**Figure E-15** The typical XPS profile for MCM-41(BMD2)-supported dMMAO exhibited the identical binding energy (BE) of Al 2p

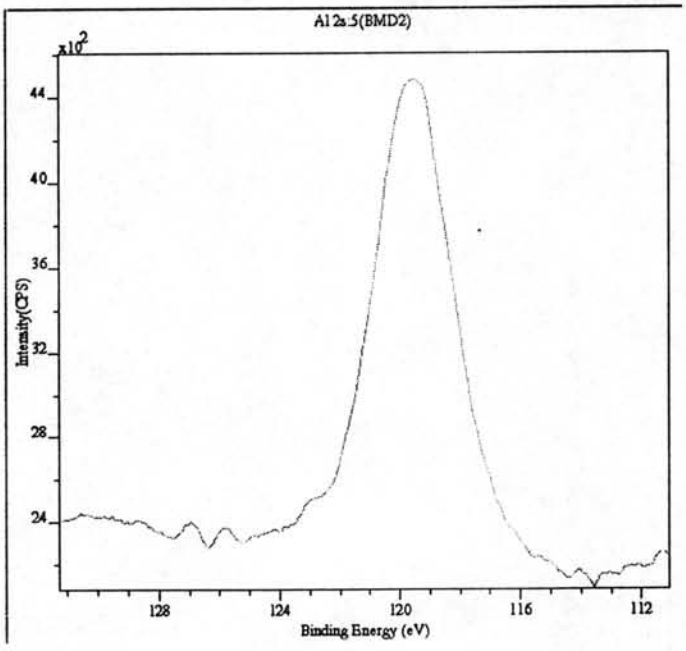


**Figure E-16** The typical XPS profile for MCM-41(BMD2)-supported dMMAO exhibited the identical binding energy (BE) of Al 2s

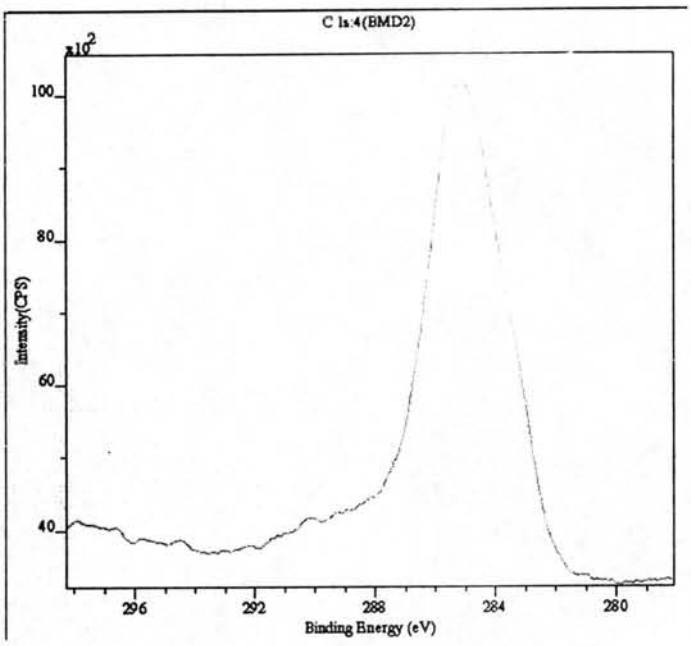


**Figure E-17** The typical XPS profile for MCM-41(BMD2)-supported dMMAO exhibited the identical binding energy (BE) of C 1s

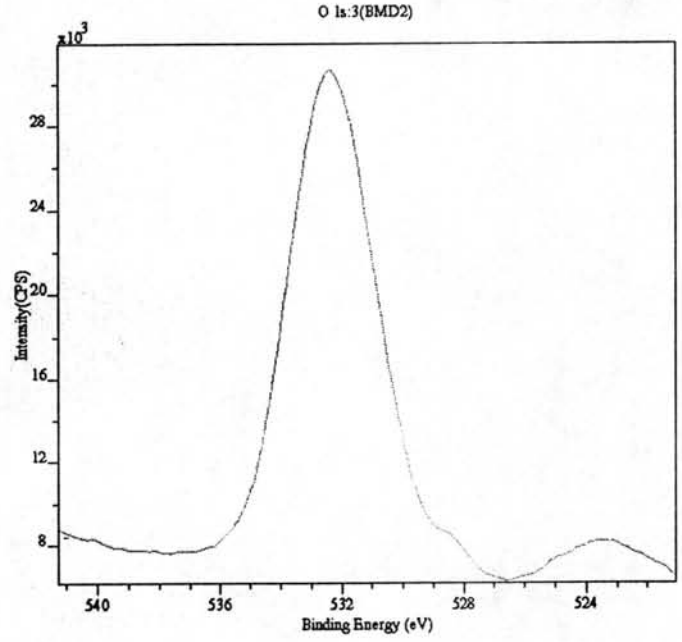


**Figure E-18** The typical XPS profile for MCM-41(BMD2)-supported dMMAO exhibited the identical binding energy (BE) of O 1s

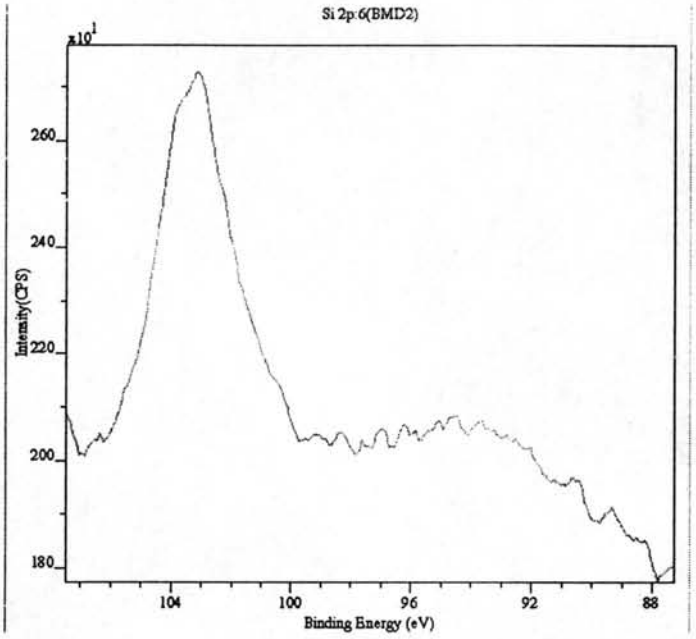


**Figure E-19** The typical XPS profile for MCM-41(BMD2)-supported dMMAO exhibited the identical binding energy (BE) of Si 2p

# APPENDIX F
# (Energy dispersive x-ray spectroscopy)

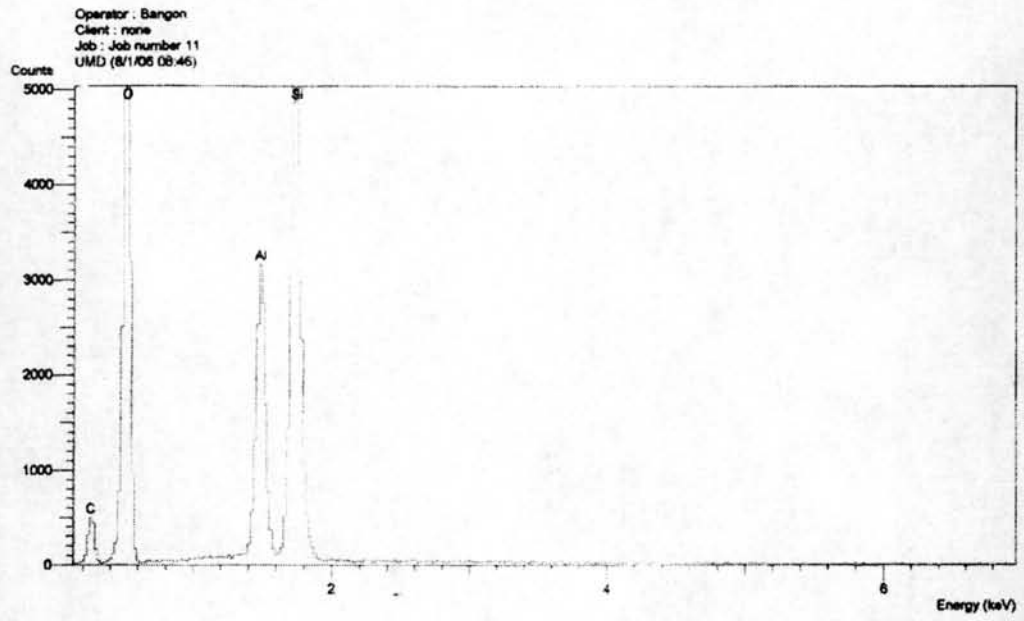


**Figure F-1** EDX profiles of $[Al]_{dMMAO}$ on MCM-41(UMD) supports

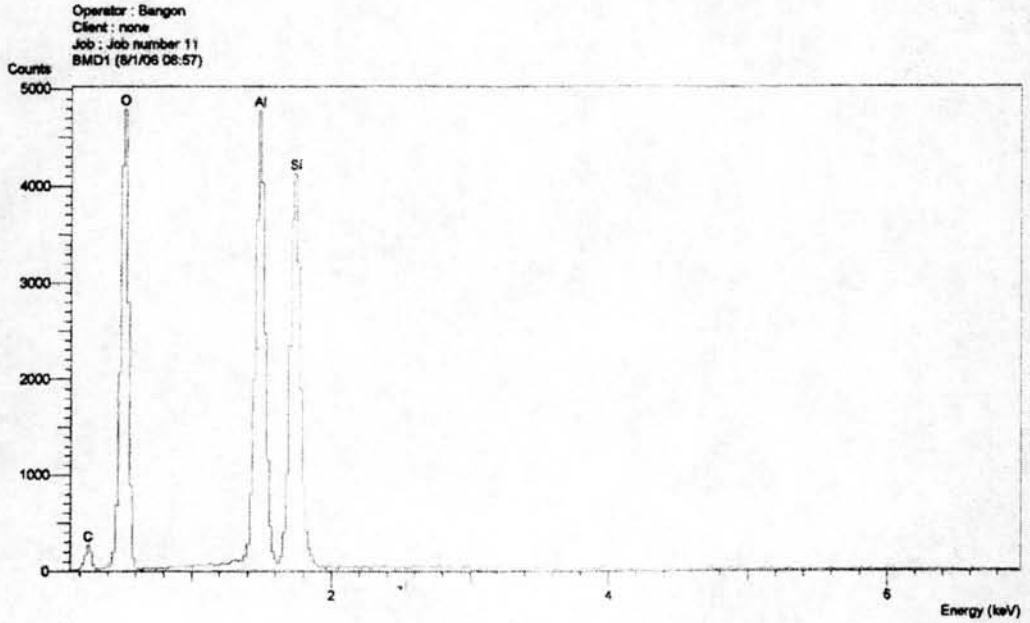


**Figure F-2** EDX profiles of $[Al]_{dMMAO}$ on MCM-41(BMD1) supports

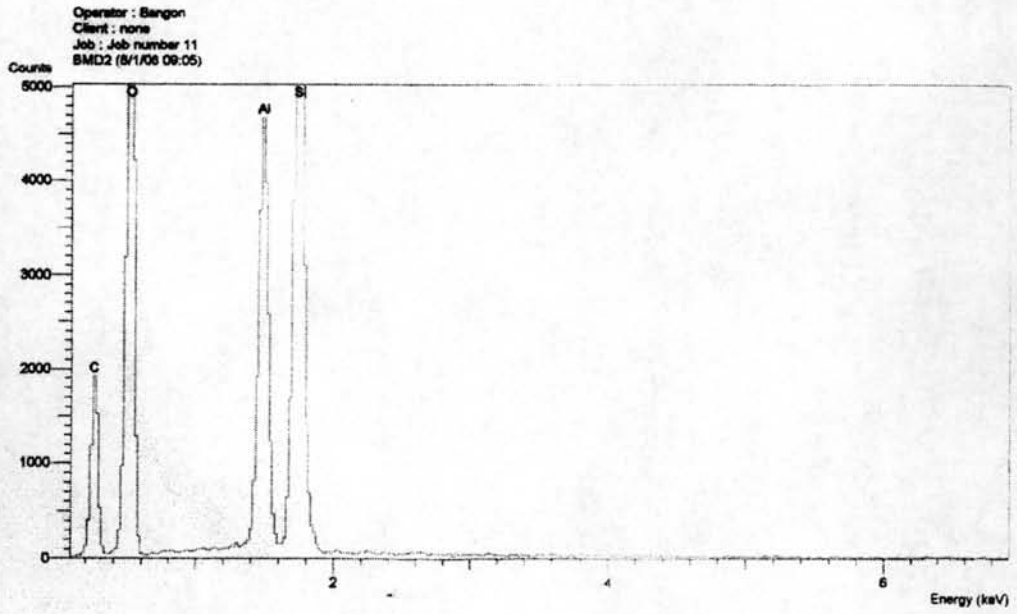


**Figure F-3** EDX profiles of $[Al]_{dMMAO}$ on MCM-41(BMD2) supports

# APPENDIX G
# (Calculation of polymer properties)

## G-1 Calculation of polymer microstructure

Polymer microstructure and also triad distribution of monomer can be calculated according to the Prof. James C. Randall [87] in the list of reference. The detail of calculation for ethylene/α-olefin copolymer was interpreted as follow.

### 1-Hexene

The integral area of $^{13}$C-NMR spectrum in the specify range are listed.

| | | | |
|---|---|---|---|
| $T_A$ | = | 39.5 - 42 | ppm |
| $T_B$ | = | 38.1 | ppm |
| $T_C$ | = | 33 - 36 | ppm |
| $T_D$ | = | 28.5 - 31 | ppm |
| $T_E$ | = | 26.5 – 27.5 | ppm |
| $T_F$ | = | 24 - 25 | ppm |
| $T_G$ | = | 23.4 | ppm |
| $T_H$ | = | 14.1 | ppm |

Triad distribution was calculated as the followed formula.

| | | |
|---|---|---|
| k[HHH] | = | $2T_A - T_C + T_G + 2T_F + T_E$ |
| k[EHH] | = | $2T_C - 2T_G - 4T_F - 2T_E - 2T_A$ |
| k[EHE] | = | $T_B$ |
| k[EEE] | = | $0.5T_D - 0.5T_G - 0.25T_E$ |
| k[HEH] | = | $T_F$ |
| k[HEE] | = | $T_E$ |

**1-Octene**

The integral area of $^{13}$C-NMR spectrum in the specify range are listed.

| | | | |
|---|---|---|---|
| $T_A$ | = | 39.5 - 42 | ppm |
| $T_B$ | = | 38.1 | ppm |
| $T_C$ | = | 36.4 | ppm |
| $T_D$ | = | 33 - 36 | ppm |
| $T_E$ | = | 32.2 | ppm |
| $T_F$ | = | 28.5 - 31 | ppm |
| $T_G$ | = | 25.5 - 27.5 | ppm |
| $T_H$ | = | 24 - 25 | ppm |
| $T_I$ | = | 22 - 23 | ppm |
| $T_J$ | = | 14 – 15 | ppm |

Triad distribution was calculated as the followed formula.

| | | |
|---|---|---|
| k[OOO] | = | $T_A - 0.5T_C$ |
| k[EOO] | = | $T_C$ |
| k[EOE] | = | $T_B$ |
| k[EEE] | = | $0.5T_F - 0.25T_E - 0.25T_G$ |
| k[OEO] | = | $T_H$ |
| k[OEE] | = | $T_G - T_E$ |

**1-Decene**

The integral area of $^{13}$C-NMR spectrum in the specify range are listed.

| | | | |
|---|---|---|---|
| $T_A$ | = | 39.5 - 42 | ppm |
| $T_B$ | = | 38.1 | ppm |
| $T_C$ | = | 36.4 | ppm |
| $T_D$ | = | 33 - 36 | ppm |
| $T_E$ | = | 32.2 | ppm |
| $T_F$ | = | 28.5 - 31 | ppm |
| $T_G$ | = | 25.5 - 27.5 | ppm |
| $T_H$ | = | 24 - 25 | ppm |
| $T_I$ | = | 22 - 23 | ppm |
| $T_J$ | = | 14 – 15 | ppm |

Triad distribution was calculated as the followed formula.

| | | |
|---|---|---|
| k[DDD] | = | $T_A - 0.5T_C$ |
| k[EDD] | = | $T_C$ |
| k[EDE] | = | $T_B$ |
| k[EEE] | = | $0.5T_F - 0.5T_E - 0.5T_G - T_I$ |
| k[DED] | = | $T_H$ |
| k[DEE] | = | $T_G - T_I$ |

All copolymer was calculated for the relative comonomer reactivity ($r_E$ for ethylene and $r_C$ for the comonomer) and monomer insertion by using the general formula below.

$$r_E = 2[EE]/([EC]X) \qquad r_C = 2[CC]X/[EC]$$

where $r_E$ = ethylene reactivity ratio

$r_C$ = comonomer ($\alpha$ -olefin) reactivity ratio

[EE] = [EEE] + 0.5[CEE]

[EC] = [CEC] + 0.5[CEE] + [ECE] + 0.5[ECC]

[CC] = [CCC] + 0.5[ECC]

X = [E]/[C] in the feed = concentration of ethylene (mol/L) / concentration of comonomer (mol/L) in the feed.

%E = [EEE] + [EEC] + [CEC]

%C = [CCC] + [CCE] + [ECE]

**APPENDIX H**
(Research output)

# Impact of MCM-41 pore structure on ethylene/1-octene copolymerization using MCM-41-supported dried MMAO with zirconocene catalyst

Sirinlak Bunchongturakarn, Bunjerd Jongsomjit* and Piyasan Praserthdam

*Center of Excellence on Catalysis and Catalytic Reaction Engineering*
*Department of Chemical Engineering, Faculty of Engineering*
*Chulalongkorn University, Bangkok 10330 Thailand*

*Corresponding author, E-mail: bunjerd.j@chula.ac.th

## ABSTRACT

MCM-41 with different pore structure was synthesized and investigated with X-ray diffraction (XRD) and $N_2$ physisorption. The ethylene/1-octene copolymerization was carried out with the MCM-41-supported dried MMAO using zirconocene catalyst. It was found that MCM-41 with bimodal pore size distribution had higher catalytic activity for ethylene/1-octene copolymerization than the unimodal one. This showed that the pore structure of MCM-41 had effect on ethylene/1-octene copolymerization.

## 1. INTRODUCTION

MCM-41 is known as a well defined and designable mesoporous material with narrow pore size distribution, large internal surface area and hexagonal arrangament of uniformly sized cylindrical pore ( 15 to 100 Å )[1,2]. Their pore dimeters are larger compared to common zeolites enabling large metallocene molecules to be immobilized not only onto the surface but also inside the pore of supports. Furthermore, the geometrical shape of the nano-channels can serve as polymerization reactors to affect the pattern and activity of monomer insertion and to control polymer chain arrangement and polymer morphology [3]. Many researchers are interested in obtaining bimodal polyethylenes using bicomponent catalyst or support [4,5]

In this present work, polyethylene were prepared via ethylene/1-octene copolymerization using MCM-41-supports with zirconocene catalyst. The influence of various pore structures of MCM-41 on catalytic activity was investigated and compared in detail.

## 2. EXPERIMENTAL

The ethylene and 1-octene copolymerization reaction were carried out in a 100 ml semi-batch stainless steel auto clave reactor equipped with magnetic stirrer. In the glove box The amount of $Et(Ind)_2ZrCl_2$ and TMA were mixed and stirred for 5 minutes at room temperature, then toluene ( to make a total volume of 30 ml ), 100 mg of catalyst precursor were introduced into the autoclave. After that the mixture of $Et(Ind)_2ZrCl_2$ and TMA was injected into the reactor. The reactor was frozen in liquid nitrogen to stop reaction and then the autoclave was evacuated to remove the argon. After that, the reactor was heated up to polymerization temperature and the polymerization was started by feeding ethylene gas ( total pressure 50 psi ) until the

consumption of ethylene 0.018 mol ( 6 psi was observed from pressure gauge ). The reaction of polymerization was terminated by addition of acidic methanol. The time of reaction was recorded for purposes of calculating the activity. The precipitated polymer was washed with methanol and dried in room temperature.

## 3. RESULTS AND DISCUSSION

The catalytic activities are listed in Table1. According to the heterogeneous system, it was found that the catalytic activities of ethylene/1-octene copolymerization using the bimodal MCM-41 support was higher than the unimodal one.The amount of Al (MMAO) at surface was determined by XPS and EDX measurement. The result indicated that both unimodal and bimodal MCM-41 gave similar amounts of MMAO at surface. It can be concluded that the pore structure of MCM-41 had effect on interaction between Al (MMAO) and supports for ethylene/ 1-octene copolymerization.

**Table 1**
Catalytic activities during ethylene/1-octene copolymerization via MCM-41-supported MMAO with zirconocene catalyst

| System | Polymerization time (s) | Polymer yield [a] (g) | Catalytic activity [b] ($\times 10^{-4}$ kg polymer $mol^{-1}$ Zr.h ) |
|---|---|---|---|
| Homogeneous | 87 | 1.59 | 4.39 |
| UMD[c] | 186 | 1.58 | 2.04 |
| BMD1[d] | 145 | 1.58 | 2.62 |
| BMD2 [e] | 150 | 1.54 | 2.47 |

[a] The polymer yield was fixed [limited by ethylene fed and 1-octene used (0.018 mole equally)]
[b] Activities were measured at polymerization temperature of 70 °C, [Ethylene]=0.018 mole, $[Al]_{MMAO}/[Zr]$ = 1135, $[Al]_{TMA}/[Zr]$ = 2500, in toluene with volume = 30 ml, and [Zr] = $5\times10^{-5}$M
[c] MCM-41 with unimodal pore size distribution
[d] MCM-41 with bimadal pore size distribution (distribution of each size was not equal )
[e] MCM-41 with bimadal pore size distribution (distribution of each size was equal )

**Reference**

1. **Beck, J.S.** (1992). *A New Family of Mesoporous Molecular Sieves Prepared with Liquid Crystal Templates.* J. Am. Chem. Soc. 114, 10834-10843.

2. **Young Soo Ko.** (2001). *Copolymerization of Ethylene and α-Olefin Using $Et(Ind)_2Zr_2Cl_2$ Entrapped inside the Regular and Small Pores of MCM-41.* Macromol. Chem. Phys. 202, 739-744.

3. **Xiaochen Dong.** (2005). *MCM-41 and SBA-15 supported $Cp_2ZrCl_2$ catalysts for the preparation of nano-polyethylene fibers via in situ ethylene extrusion polymerization.* Journal of Molecular Catalysis A: Chemical. 240, 239-244.

4. **Chengbin Liu.** (2003). *Zirconocene catalyst well spaced inside modified montmorillonite for ethylene polymerization: role of pretreatment and modification of montmorillonite in tailoring polymer properties.* Journal of catalysis. 221, 162-169.

5. **Yi Zhang.** (2002). *Simultaneous introduction of chemical and spatial effect via a new bimodal catalyst support preparation method.* Chem. Commun. 1216-1217.

# Impact of bimodal pore MCM-41-supported zirconocene/dMMAO catalyst on copolymerization of ethylene/1-octene

Sirinlak Bunchongturakarn, Bunjerd Jongsomjit* and Piyasan Praserthdam

Center of Excellence on Catalysis and Catalytic Reaction Engineering

Department of Chemical Engineering, Faculty of Engineering

Chulalongkorn University, Bangkok 10330 Thailand

*Corresponding author, **E-mail:** bunjerd.j@chula.ac.th

**Tel:** 662-2186869, **Fax:** 662-2186877

## Abstract

The bimodal MCM-41-supported zirconocene/dMMAO catalyst exhibited higher catalytic activity for ethylene/1-octene copolymerization compared to the unimodal one. The higher activity can be attributed to lesser support interaction. The copolymer having broader MWD was obtained with the bimodal support without any significant changes in MW and polymer microstructure as seen by $^{13}C$ NMR.

**Keywords:** MCM-41; bimodal support; metallocene catalyst; support interaction; polyolefins

## 1. Introduction

For years, the correlation between metallocene structure and polymerization behaviors for olefin polymerization have been extensively studied and developed consistently. In general, metallocenes are single site catalysts producing polymers having narrow molecular weight distribution (MWD) and homogeneously chemical composition [1,2]. However, it is found that the homogeneous metallocene catalytic system has two major disadvantages; the lack of morphology control of polymer causing the reactor fouling and the limitation of being able to use only in the solution process whereas the existing technologies are mainly based on the gas phase and slurry processes. Therefore, binding these metallocene catalysts onto suitable inorganic supports can provide a promising way to overcome those drawbacks.

Several studies [3-9] have been concentrated on the use of supported metallocene catalyst for the olefin polymerization. Apparently, silica, alumina and magnesia supports have been the most widely used inorganic supports so far. The aim is to develop a way to attach the metallocene to the support without losing the performance of the homogeneous complex. The main immobilization techniques can be performed by direct impregnation of metallocene or cocatalyst on the support, then pretreatment of the support followed by activation of metallocene. Hence, high surface area and the presence of well-defined, stable sites for the attachment of the active component to the support are very crucial [10].

As well known, a new class of mesoporous silica tube-like materials designated as MCM-41 was introduced in 1992 [11,12]. The MCM-41 is recognized as a well-defined as mesoporous material with narrow pore size distribution, large internal surface area, distinct adsorption properties and hexagonal arrangement of uniformly sized cylindrical pore. It has the possibility to control the internal diameter of mesopores between 15 and

100 Å by varying the chain length of the micellar surfactant template. In fact, its pore diameter can enable large metallocene molecules to be immobilized onto both the surface and inside the pore. These excellent properties of this material essentially emulate researchers to use the MCM-41 as the support for metallocene catalysts for olefin polymerization [13-19].

In general, the surface areas mainly control the dispersion of supported metal. As a matter of fact, too large surface area (small pore diameter) results in poor diffusion efficiency of reactant and products in the intra-pellet structure whereas a catalyst having too large pore diameter exhibits a small surface area leading to low metal dispersion and low catalytic activity. A support with a distinct bimodal structure has excellent advantages for solving the contradiction as mentioned before. In particular, the large pores provide rapid transportation of reactant and product molecules whereas the small pores render a large surface area. Moreover, the geometrical shape of the nano-channels of support can serve as polymerization reactors to affect the pattern and activity of monomer insertion. Thus, the arrangement of polymer chain and polymer morphology can be controlled. Many researchers are interested in obtaining bimodal polyethylene using bicomponent catalyst or support [20-22].

In this present study, the MCM-41 supports having different pore size distribution such as unimodal and bimodal pore sizes were synthesized. Then, the linear low-density polyethylene (LLDPE) was prepared by ethylene/1-octene copolymerization using various unimodal and bimodal MCM-41-supported zirconocene/dMMAO catalysts. The influences of various pore structures of MCM-41 on the catalytic activity and polymer properties were investigated. The copolymers obtained were further analyzed using GPC and $^{13}C$ NMR.

## 2. Experimental

### 2.1 Materials

All chemicals and polymerization were manipulated under an argon atmosphere, using a glove box and/or Schlenk techniques. Toluene was dried over dehydrated $CaCl_2$ and distilled over sodium/benzophenone before use. The *rac*-ethylenebis (indenyl) zirconium dichloride (*rac*-Et[Ind]$_2$Zr$Cl_2$) was supplied from Aldrich Chemical Company, Inc. Modified methylaluminoxane (MMAO) in hexane was donated by Tosoh (Akso, Japan). Trialkylaluminum (TMA, 2 M in toluene) was supplied by Nippon Aluminum Alkyls, Ltd., Japan. Ultrahigh purity argon was further purified by passing it through columns that were packed with BASF catalyst R3-11G (molecular-sieved to 3 Å), sodium hydroxide (NaOH), and phosphorus pentaoxide ($P_2O_5$) to remove traces of oxygen and moisture. Ethylene gas (99.96% pure) was donated by the National Petrochemical Co., Ltd., Thailand. 1-Octene (d = 0.715) was purchased from Aldrich Chemical Company, Inc.

### 2.2 Preparation of bimodal MCM-41 support

The MCM-41 support was synthesized according to the method described by Panpranot et al. [23] using the gel composition of CTABr : 0.3 $NH_3$ : 4 $SiO_2$ : $Na_2O$ : 200 $H_2O$, where CTABr denotes cetyltrimethyl ammonium bromide. Briefly, 20.03 g of colloidal silica Ludox HS 40 % (Aldrich Chemical Company, Inc.) was mixed with 22.67 g of 11.78 % sodium hydroxide solution. Another mixture comprised of 12.15 g of CTABr (Aldrich Chemical Company, Inc.) in 36.45 g of deionized water, and 0.4 g

of an aqueous solution of 25 % $NH_3$. Both of these mixture were stirred by agitator for 30 min, then heated statically at 373 K for 5 days. The obtained solid material was filtered, washed with deionized water until no base was detected and then dried at 373 K. The sample was then calcined in flowing nitrogen up to 823 K (1-2 K/min), then in air at the same temperature for 5 h. After preparation, the unimodal MCM-41 support (denoted as UMD) having the pore diameter of ca. 2 nm and surface area of 864 $m^2/g$ was obtained. The bimodal MCM-41 having average pore diameters of ca. 5 and 6 nm (denoted as BMD1 and BMD2, respectively) was prepared by treating the UMD-MCM-41 (before calcination) with an emulsion containing *N,N*-dimethyl decylamine (0.625 g in 37.5 g of water for each gram of MCM-41) for 3 and 4 days at 393 K. This was washed thoroughly, dried and calcined in flowing nitrogen up to 823 K (1-2 K/min), then in air at the same temperature for 5 h.

### 2.3 Preparation of dried-MMAO (dMMAO)

Removal of TMA from MMAO was carried out according to the reported procedure [24]. The toluene solution of MMAO was dried under vacuum for 6 h at room temperature to evaporate the solvent, TMA, and Al(*i*Bu)$_3$ (TIBA). Then, continue to dissolve with 100 ml of heptane and the solution was evaporated under vacuum to remove the remaining TMA and TIBA. This procedure was repeated 4 times and the white powder of dried MMAO (dMMAO) was obtained.

### 2.4 Preparation of MCM-41-supported dMMAO

The MCM-41 support was reacted with the desired amount of dMMAO in 20 ml of toluene at room temperature for 30 min. The solvent was then removed from the

mixture by evacuated. This procedure was done only once with toluene (20 ml x 1) and 3 times with hexane (20 ml x 3). Then, the solid part was dried under vacuum at room temperature. The white powder of supported cocatalyst (dMMAO/support) was then obtained.

## 2.5 Polymerization

The ethylene/1-octene copolymerization reaction was carried out in a 100 ml semi-batch stainless steel autoclave reactor equipped with magnetic stirrer. In the glove box, the desired amounts of *rac*-Et[Ind]$_2$ZrCl$_2$ and TMA were mixed and stirred for 5 min for aging. Then, toluene (to make a total volume of 30 ml) and 100 mg of dMMAO/support were introduced into the reactor. After that, the mixture of *rac*-Et[Ind]$_2$ZrCl$_2$ and TMA were injected into the reactor. The reactor was frozen in liquid nitrogen to stop reaction and then 0.018 mol of 1-octene was injected into the reactor. The reactor was evacuated to remove argon. Then, it was heated up to polymerization temperature (343 K) and the polymerization was started by feeding ethylene gas (total pressure 50 psi in the reactor) until the consumption of ethylene 0.018 mol (6 psi was observed from the pressure gauge) was reached. The reaction of polymerization was completely terminated by addition of acidic methanol. The time of reaction was recorded for purpose of calculating the activity. The precipitated polymer was washed with methanol and dried at room temperature.

## 2.6 Characterization

### 2.6.1 Characterization of supports and catalyst precursor

*$N_2$ physisorption*: Measurement of BET surface area, average pore diameter and pore size distribution of MCM-41 support were determined by $N_2$ physisorption using a Micromeritics ASAP 2000 automated system.

*X-ray diffraction*: XRD was performed to determine the bulk crystalline phases of samples. It was conducted using a SIEMEN D-5000 X-ray diffractometer with $CuK_\alpha$ ($\lambda$ = 1.54439 Å). The spectra were scanned at a rate of 2.4° $min^{-1}$ in the range of $2\theta$ = 10-80°.

*Scanning electron microscopy and energy dispersive X-ray spectroscopy*: SEM and EDX were used to determine the morphologies and elemental distribution throughout the sample granules, respectively. The SEM of JEOL mode JSM-6400 was applied. The EDX was performed using Link Isis series 300 program.

*Raman spectroscopy*: The Raman spectra of the samples were collected by projecting a continuous wave YAG laser of Nd (810 nm) through the samples at room temperature. A scanning range of 100-1000 $cm^{-1}$ with a resolution of 2 $cm^{-1}$ was applied.

*X-ray photoelectron spectroscopy*: XPS was used to determine the binding energies (BE) and surface concentration of samples. It was carried out using the Shimazu AMICUS with VISION 2-control software. Spectra were recorded at room temperature in high-resolution mode (0.1 eV step, 23.5 eV pass energy) for Al 2p core-level region. The samples were mounted on an adhesive carbon tape as

pellets. The energy reference for Ag metal (368.0 eV for $3d_{5/2}$) was used for this study.

*Thermogravimetric analysis*: TGA was performed using TA Instruments SDT Q 600 analyzer. The samples of 10-20 mg and a temperature ramping from 298 to 500 K at 2 K/min were used in the operation. The carrier gas was $N_2$ UHP.

### 2.6.2 Characterization of polymer

*Gel permeation chromatography*: The molecular weight (MW) and molecular weight distribution (MWD) of polymer were determined using GPC (GPC, PL-GPC-220). Samples were prepared having approximately concentration of 1 to 2 mg/ml in trichlorobenzene (mobile phase) by using the sample preparation unit (PL-SP 260) with filtration system at a temperature of 423 K. The dissolved and filtered samples were transferred into the GPC instrument at 423 K. The calibration was conducted using the universal calibration curve based on narrow polystyrene standards.

*$^{13}C$ NMR spectroscopy:* $^{13}C$ NMR spectroscopy was used to determine the triad distribution and 1-octene insertion indicating the copolymer microstructure. Chemical shift were referenced internally to the $CDCl_3$ and calculated according to the method described by Randall [34]. Sample solution was prepared by dissolving 50 mg of copolymer in 1,2,4-trichlorobenzene and $CDCl_3$. $^{13}C$ NMR spectra were taken at 333 K using BRUKER AVANCE II 400 operating at 100 MHz with an acquisition time of 1.5 s and a delay time of 4 s.

## 3. Results and discussion

### 3.1 Catalytic activity

The main focus of this present study was to investigate the impact of different pore structures of MCM-41 support on the catalytic activity during copolymer of ethylene/1-octene with MCM-41-supported zirconocene/dMMAO catalyst. First, the MCM-41 supports having different pore structures were prepared based on different pretreatment conditions. After preparation of supports, the unimodal MCM-41 support denoted as UMD having the average pore diameter of ca. 2 nm and surface area of 883.5 $m^2/g$ was obtained as seen in **Table 1**. The pore size distribution of the MCM-41 (UMD) is shown in **Figure 1** indicating only the unimodal pore size distribution. By treating the MCM-41 (UMD) with *N,N*-dimethyldecylamine at the specified conditions, the bimodal MCM-41 supports denoted as BMD can be achieved. The BMD1 is assigned to the bimodal MCM-41 support having the average pore diameter of ca. 5 nm (surface area = 400.3 $m^2/g$) whereas the BMD2 refers to the bimodal MCM-41 with the average pore diameter of ca. 6 nm (surface area = 400.0 $m^2/g$) as also shown in **Table 1** and **Figure 1**. As seen in **Figure 1**, it can be observed that the MCM-41 (BMD2) support exhibited larger portion of the large pore than the MCM-41 (BMD1) one. The XRD patterns of various MCM-41 supports are shown in **Figure 2**. It can be seen that all MCM-41 supports gave the similar XRD patterns consisting of a broad peak of amorphous silica around 20 to 30°. As confirmation, no significantly different Raman bands **(Figure 3)** were also

observed for all MCM-41 supports within the Raman shift ranged between 200 and 1000 $cm^{-1}$.

After impregnation with dMMAO, the nature and surface concentrations of $[Al]_{dMMAO}$ on various MCM-41 supports were determined using the XPS measurement. The typical XPS profile (not shown) for all MCM-41-supported dMMAO exhibited the identical binding energy (BE) of Al 2p at ca. 74.6-74.7 eV. It should be noted that the BE for Al 2p obtained here was also in accordance with that on silica as reported by Hagimoto et al. [24]. Thus, it indicated that no transformation of the oxidation state for the cocatalyst (dMMAO) present on various MCM-41 supports employed. The surface concentrations of $[Al]_{dMMAO}$ measured by XPS are also shown in **Table 2**. It can be observed that the surface concentrations of $[Al]_{dMMAO}$ were similar for both MCM-41 (BMD) supports having $[Al]_{dMMAO}$ at surface of 27.0 wt%. However, it appeared that the MCM-41 (UMD) support had a slightly higher amount of $[Al]_{dMMAO}$ at surface (27.3 wt%) than that of the MCM-41 (BMD) support. Besides the amounts of $[Al]_{dMMAO}$ surface concentration, one should consider the distribution of the cocatalyst on the various supports. Therefore, the elemental distribution for $[Al]_{dMMAO}$ was also performed using EDX mapping on the external surface of the catalyst precursors. The $[Al]_{dMMAO}$ distribution on various supports is shown in **Figure 4**. As seen, all samples exhibited good distribution of Al without any changes in the support morphology.

The catalytic activities via various MCM-41 supports and the homogeneous system are listed in **Table 3**. It was obvious that the homogeneous catalytic system provided the highest activity among the supported system due to the absence of supporting effect [5,8,9]. Considering the various MCM-41-supported systems, it

was found that the MCM-41 (BMD) rendered higher activity than the UMD one about 1.2-1.5 times. Although the amount of $[Al]_{dMMAO}$ at surface of the MCM-41 (UMD) as measured by XPS was slightly higher, the catalytic activity was lower. It is known that besides the concentrations of active species, one should consider on the interaction between the active species and support. In fact, too strong interaction can result in compound formation at surface [25-29] and/or inactive species leading to low catalytic activity. A wide range of variables including nature of supports and active species, particle size, and treatment conditions can affect the degree of support interaction. Essentially, they can be superimposed on each other. However, based on this study, the active species ($[Al]_{dMMAO}$) present on different MCM-41 supports had the similar characteristics of Al 2p as measured by XPS indicating that no other compound formation on surface was formed. Thus, it was suggested that based on the similar amount of $[Al]_{dMMAO}$ added, the size of the $[Al]_{dMMAO}$ present in the small pore [MCM-41 (UMD)] was presumably smaller due to larger surface area. As a matter of fact, the smaller particle can interact more with the support resulting in stronger support interaction. In order to identify the interaction of $[Al]_{dMMAO}$ on various MCM-41 supports, the TGA measurement was performed. The TGA profiles of $[Al]_{dMMAO}$ on various MCM-41 supports are shown in **Figure** 5 indicating the similar profiles for various supports. It was observed that the weight loss of $[Al]_{dMMAO}$ present on various supports were in the order of MCM-41 (BMD1) (12.8%) > MCM-41 (BMD2) (12.2%) > MCM-41 (UMD) (11.5%). Based on TGA, it indicated that the $[Al]_{dMMAO}$ present on MCM-41 (UMD) had the strongest interaction among the other supports, thus, having the lowest polymerization activity.

It is worth noting that the higher activity obtained from the bimodal support can be attributed to the optimum interaction between the support and active species.

### 3.2 Polymer Characteristics

The various copolymers obtained were further characterized by means of GPC and $^{13}C$ NMR. The GPC was performed in order to determine the MW, $M_n$ and MWD of polymers. The GPC results are shown in **Table 4**. Considering the different catalytic systems, it can be observed that the homogeneous system exhibited higher MW than the supported system did. As known from our previous works, the supported system apparently promoted the chain transfer reaction resulting in lower MW of polymers [8,30]. Based on the supported system, it revealed that the copolymer obtained from the bimodal MCM-41 supports had broader MWD than that derived from the unimodal one. It was suggested that this broad MWD copolymer can be attributed to the different natures of catalytic sites present on the bimodal supports. However, the observed MW of copolymers among all supports was slightly different.

The quantitative analysis of triad distribution for all copolymers was conducted on the basis assignment of the $^{13}C$ NMR spectra of ethylene/1-octene (EO) copolymer [31]. The characteristics of $^{13}C$ NMR spectra (not shown) for all copolymers were similar indicating the copolymer of ethylene/1-octene. The triad distribution of all polymers is shown in **Table 5**. Ethylene incorporation in all systems gave copolymers with similar triad distribution. It was also shown a little probability to produce the block of OO, which is the characteristic of this zirconocene in homogeneous system [5]. No triblock of OOO in the copolymers was found. Only the random copolymers

can be produced in all systems. In addition, the octene incorporations in all supported systems were between 25 and 32 mol%, which was similar with that in the homogeneous system.

## 4. Conclusions

In summary, the bimodal MCM-41-supported zirconocene/dMMAO showed the enhancement of activity during copolymerization of ethylene/1-octene about 1.5 times compared with that using the unimodal one. It was proven that the higher activity could be attributed to lesser interaction between the support and cocatalyst. Besides, the bimodal MCM-41 support apparently gave broader MWD copolymer due to more different catalytic sites present. However, both unimodal and bimodal MCM-41 supports trended to produce the random copolymers with a little probability for the block of OO.

**Acknowledgements**

We thank the Thailand Research Fund (TRF) and the graduate school at Chulalongkorn University ($90^{th}$ Anniversary of CU) for financial support of this project. Guidance of the MCM-41 preparation by Dr. Panpranot is greatly appreciated.

**References**

[1] J.D. Kim, J. B.P. Soares, G.L. Rempel, J. Polym. Sci. Part A: Polym. Chem. 37 (1999) 331.

[2] J.D. Kim, J. B. P. Soares, Macromol. Rapid Commun. 20 (1999) 347.

[3] H. Rahiala, I. Beurroies, T. Eklund, K. Hakala, R. Gougeon, P. Trens, J.B. Rosenholm, J. Catal. 188 (1999) 14.

[4] K-S. Lee, C-G. Oh, J-H. Yim, S-K. Ihm, J. Mol. Catal. A: Chem. 159 (2000) 301.

[5] B. Jongsomjit, P. Kaewkrajang, S.E. Wanke, P. Praserthdam, Catal. Lett. 94 (2004) 205.

[6] B. Jongsomjit, P. Praserthdam, P. Kaewkrajang, Mater. Chem. Phys. 86 (2004) 243.

[7] B. Jongsomjit, P. Kaewkrajang, T. Shiono, P. Praserthdam, Ind. Eng. Chem. Res. 43 (2004) 7959.

[8] B. Jongsomjit, S. Ngamposri, P. Praserthdam, Catal. Lett. 100 (2005) 139.

[9] B. Jongsomjit, S. Ngamposri, P. Praserthdam, Molecules 10 (2005) 603.

[10] F. Ciardilli, A. Altomare, M. Michelotti, Catal. Today 41 (1998) 149.

[11] J.S. Beck, J.C. Vartuli, W.J. Roth, M.E. Leonowicz, C.T. Kresge, K.D. Schmitt, C.T-W. Chu, D.H. Olson, E.W. Sheppard, S.B. McCullen, J.B. Higgins, J.L. Schlenker, J. Am. Chem. Soc. 114 (1992) 10834.

[12] C.T. Kresge, M.E. Leonowicz, W.J. Roth, J.C. Vartuli, J.S. Beck, Nature 359 (1992) 710.

[13] Y.S. Ko, S.I. Woo, Macromol. Chem. Phys. 202 (2001) 739.

[14] Z. Ye, S. Zhu, W.J. Wang, H. Alsyouri, Y.S. Lin, J. Polym. Sci. Part B: Polym. Phys. 41 (2003) 2433.

[15] D.E.B. Lopes, M.V. Marques, M.L. Dias, M.R. Ribeiro, J.P. Lourenco, Eur. Polym. J. 40 (2004) 2555.

[16] X.C. Dong, L. Wang, W.Q. Wang, H.J. Yu, J.F. Wang, T. Chen, Z.R. Zhao, Eur. Polym. J. 41 (2005) 797.

[17] S.T. Chen, C.Y. Guo, L. Liu, H. Xu, J.X. Dong, Y.L. Hu, Polymer 46 (2005) 11093.

[18] X.C. Dong, L. Wang, G.H. Jiang, Z.R. Zhao, T.X. Sun, H.J. Yu, W.Q. Wang, J. Mol. Catal. A: Chem. 240 (2005) 239.

[19] X.C. Dong, L. Wang, J.J. Wang, J.F. Zhou, T.X. Sun, J. Phys. Chem. B. 110 (2006) 9100.

[20] A. Reb, H.G. Alt, J. Mol. Catal. A: Chem. 174 (2001) 35.

[21] J.D. Kim, J.B.P. Soares, J. Polym. Sci. Part A: Polym. Chem. 38 (2000) 1427.

[22] Q. Wang, H.X. Yang, Z.Q. Fan, Macromol. Rapid Commun. 23 (2002) 639.

[23] J. Panpranot, K. Pattamakomsan, J.G. Goodwin Jr., P. Praserthdam, Catal. Commun. 5 (2004) 583.

[24] H. Hagimoto, T. Shiono, T. Ikeda, Macromol. Chem. Phys. 205 (2004) 19.

[25] B. Jongsomjit, J. Panpranot, J.G. Goodwin, Jr., J. Catal. 204 (2001) 98.

[26] B. Jongsomjit, J.G. Goodwin, Jr., Catal. Today 77 (2002) 191.

[27] B. Jongsomjit, J. Panpranot, J.G. Goodwin, Jr., J. Catal. 215 (2003) 66.

[28] B. Jongsomjit, C. Sakdamnuson, P. Praserthdam, Catal. Lett. 94 (2004) 209.

[29] T. Wongsalee, B. Jongsomjit, P. Praserthdam, Catal. Lett. 108 (2006) 55.

[30] B. Jongsomjit, S. Ngamposri, P. Praserthdam, Ind. Eng. Chem. Res. 44 (2005) 9059.

[31] J.C. Randall, J.Macromol. Sci., Rev. Macromol. Chem. Phys. C29 (1989) 201.

**Table 1**

BET surface area and average pore diameter of various MCM-41 supports

| Support | BET surface area ($m^2/g$) | Average pore diameter (nm) |
|---|---|---|
| MCM-41(UMD) | 863.5 | 2.3 |
| MCM-41(BMD1) | 400.3 | 4.6 |
| MCM-41(BMD2) | 400.0 | 5.7 |

**Table 2**

XPS results for different supports

| Support | BE for Al 2p[a] (eV) | Mass Concentration (%) of Al |
|---|---|---|
| dMMAO/MCM-41(UMD) | 74.7 | 27.3 |
| dMMAO/MCM-41(BMD1) | 74.6 | 27.0 |
| dMMAO/MCM-41(BMD2) | 74.7 | 27.0 |

[a] Al 2p from dMMAO

**Table 3**

Catalytic activities of various MCM-41-supported dMMAO with zirconocene catalyst during ethylene/1-octene copolymerization

| System | Polymerization time (s) | Polymer yield[a] (g) | Catalytic activities[b] ($\times 10^{-4}$ kg Pol.mol.$Zr^{-1}$.$h^{-1}$) |
|---|---|---|---|
| Homogeneous | 87 | 1.59 | 4.38 |
| MCM-41(UMD) | 186 | 1.58 | 2.04 |
| MCM-41(BMD1) | 127 | 1.58 | 2.99 |
| MCM-41(BMD2) | 150 | 1.51 | 2.42 |

[a] The polymer yield was fixed [limited by ethylene fed and 1-octene used (0.018 mole equally)].

[b] Activities were measured at polymerization temperature of 343 K, [Ethylene] = 0.018 mole, $[Al]_{dMMAO}/[Zr]_{cat}$ = 1135, $[Al]_{TMA}/[Zr]_{cat}$ = 2500, in toluene with total volume = 30 ml and $[Zr]_{cat} = 5\times10^{-5}$ M.

**Table 4**

Molar weight (MW) and molecular weight distribution (MWD) of polymers obtained from various MCM-41-supported dMMAO with zirconocene catalyst

| System | MW[a] ($\times 10^{-4}$ g mol$^{-1}$) | $M_n$[a] ($\times 10^{-4}$ g mol$^{-1}$) | MWD[a] |
|---|---|---|---|
| Homogeneous | 3.66 | 0.69 | 5.3 |
| MCM-41(UMD) | 2.91 | 0.98 | 3.0 |
| MCM-41(BMD1) | 2.69 | 0.45 | 6.0 |
| MCM-41(BMD2) | 3.07 | 0.62 | 5.0 |

[a] Obtained from GPC and MWD was calculated from $MW/M_n$

**Table 5**

$^{13}C$ NMR analysis of ethylene/1-octene copolymer

| System | Triad distribution of copolymer | | | | | | Mol % of O in copolymer |
|---|---|---|---|---|---|---|---|
| | OOO | EOO | EOE | EEE | OEO | OEE | |
| Homogeneous | 0 | 0.077 | 0.210 | 0.414 | 0.056 | 0.244 | 29 |
| MCM-41(UMD) | 0 | 0.073 | 0.232 | 0.456 | 0.075 | 0.164 | 30 |
| MCM-41 (BMD1) | 0 | 0.096 | 0.221 | 0.408 | 0.047 | 0.228 | 32 |
| MCM-41 (BMD2) | 0 | 0.057 | 0.196 | 0.456 | 0.057 | 0.234 | 25 |

**E** refers to ethylene monomer and **O** refers to 1-octene comonomer

**Table 5**

$^{13}C$ NMR analysis of ethylene/1-octene copolymer

| System | Triad distribution of copolymer | | | | | | Mol % of O in copolymer |
|---|---|---|---|---|---|---|---|
| | OOO | EOO | EOE | EEE | OEO | OEE | |
| Homogeneous | 0 | 0.077 | 0.210 | 0.414 | 0.056 | 0.244 | 29 |
| MCM-41(UMD) | 0 | 0.073 | 0.232 | 0.456 | 0.075 | 0.164 | 30 |
| MCM-41 (BMD1) | 0 | 0.096 | 0.221 | 0.408 | 0.047 | 0.228 | 32 |
| MCM-41 (BMD2) | 0 | 0.057 | 0.196 | 0.456 | 0.057 | 0.234 | 25 |

**E** refers to ethylene monomer and **O** refers to 1-octene comonomer

## List of Figures

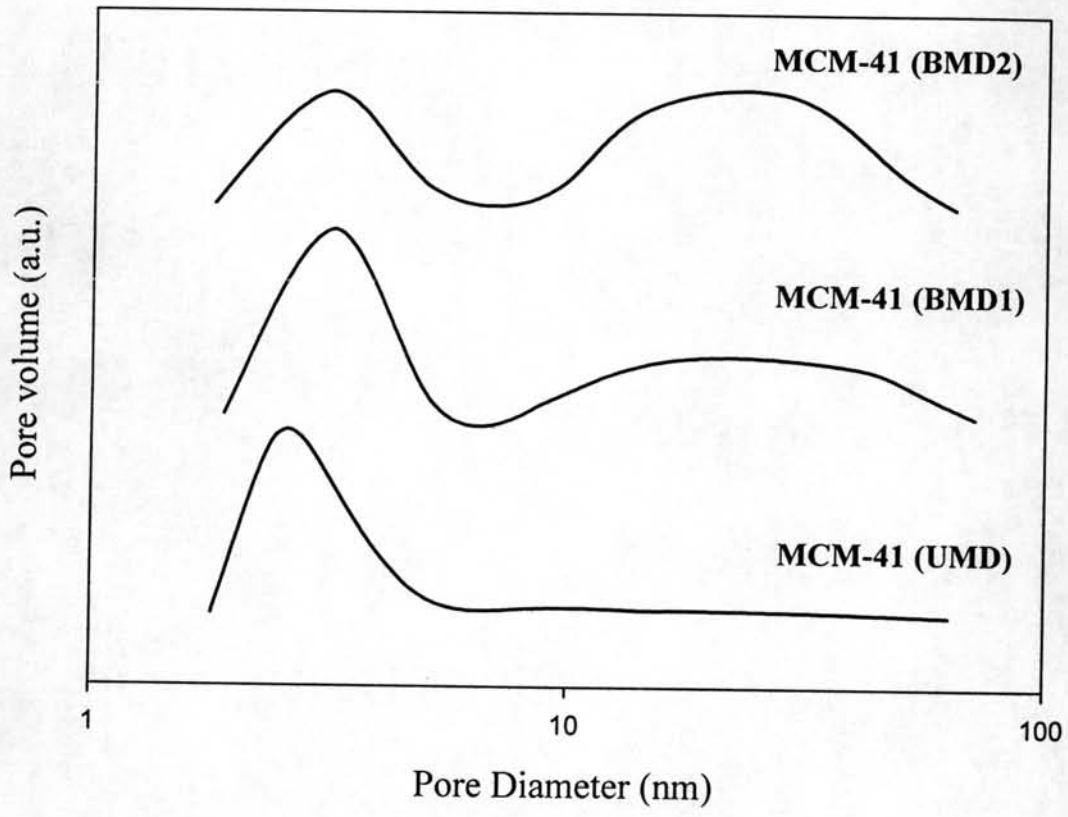
MCM-41 (BMD2)
MCM-41 (BMD1)
MCM-41 (UMD)
Pore volume (a.u.)
1
10
100
Pore Diameter (nm)

**Figure 1**

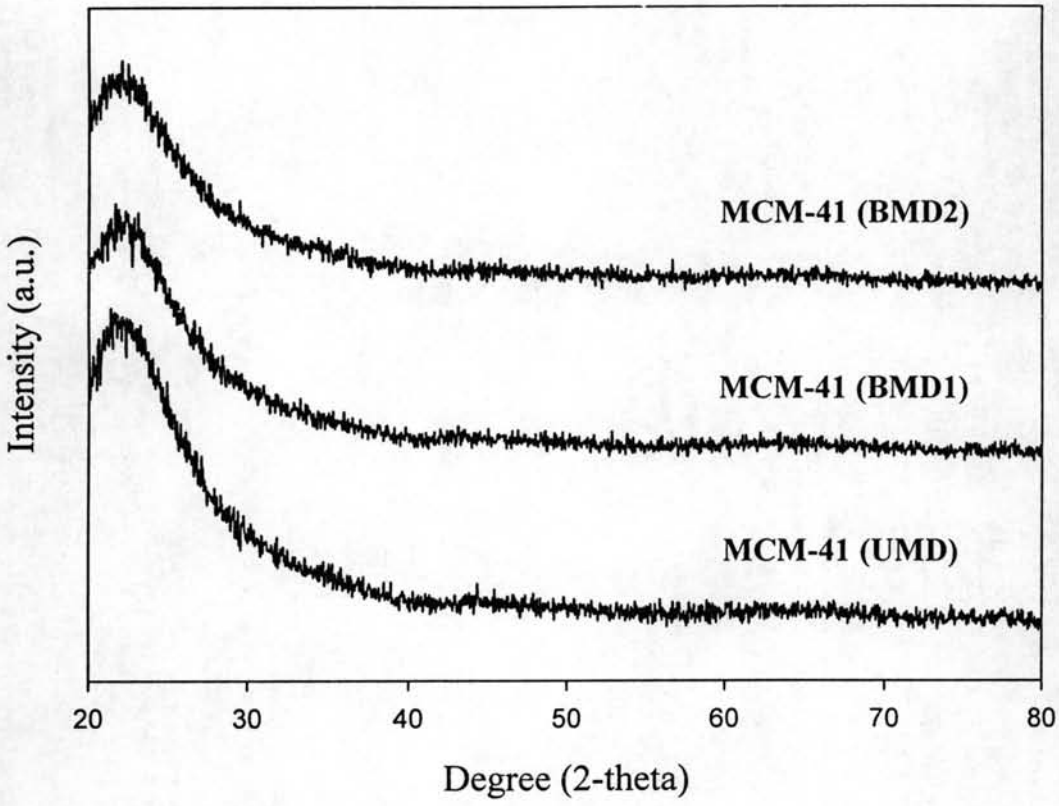
MCM-41 (BMD2)
MCM-41 (BMD1)
MCM-41 (UMD)
Intensity (a.u.)
20
30
40
50
60
70
80
Degree (2-theta)

**Figure 2**

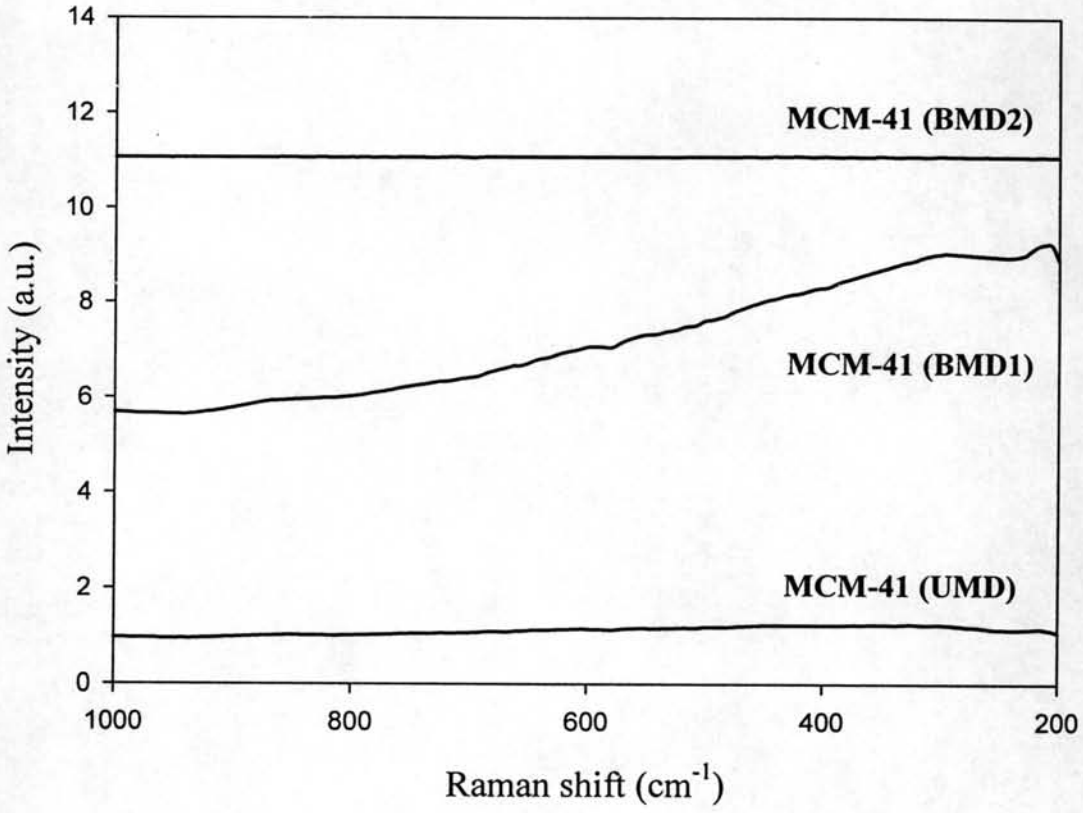
14
12
10
8
6
4
2
0
Intensity (a.u.)
MCM-41 (BMD2)
MCM-41 (BMD1)
MCM-41 (UMD)
1000
800
600
400
200
Raman shift (cm-1)

**Figure 3**

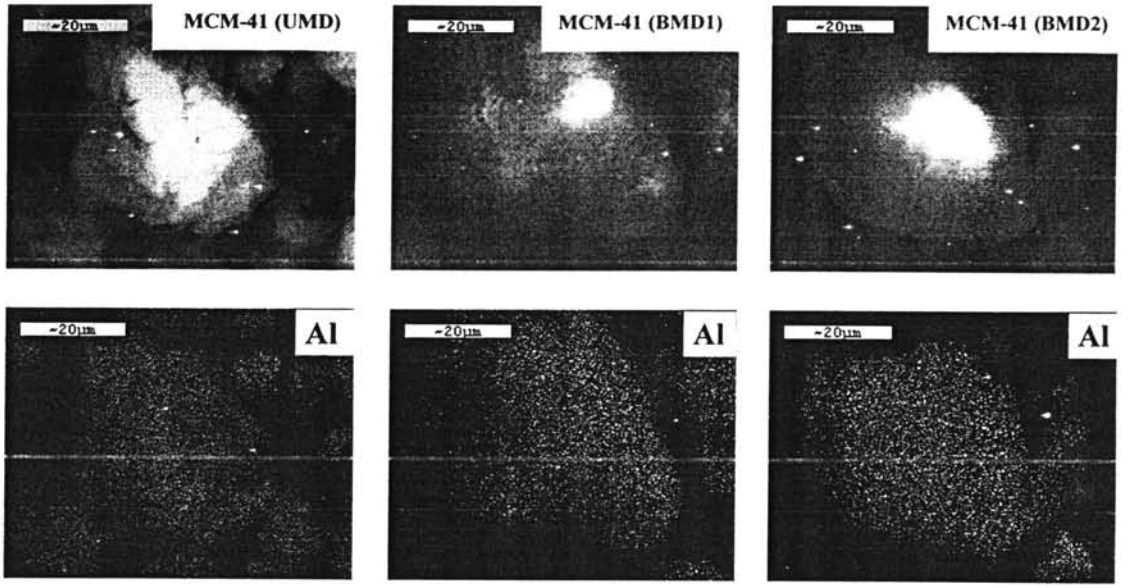


**Figure 4**

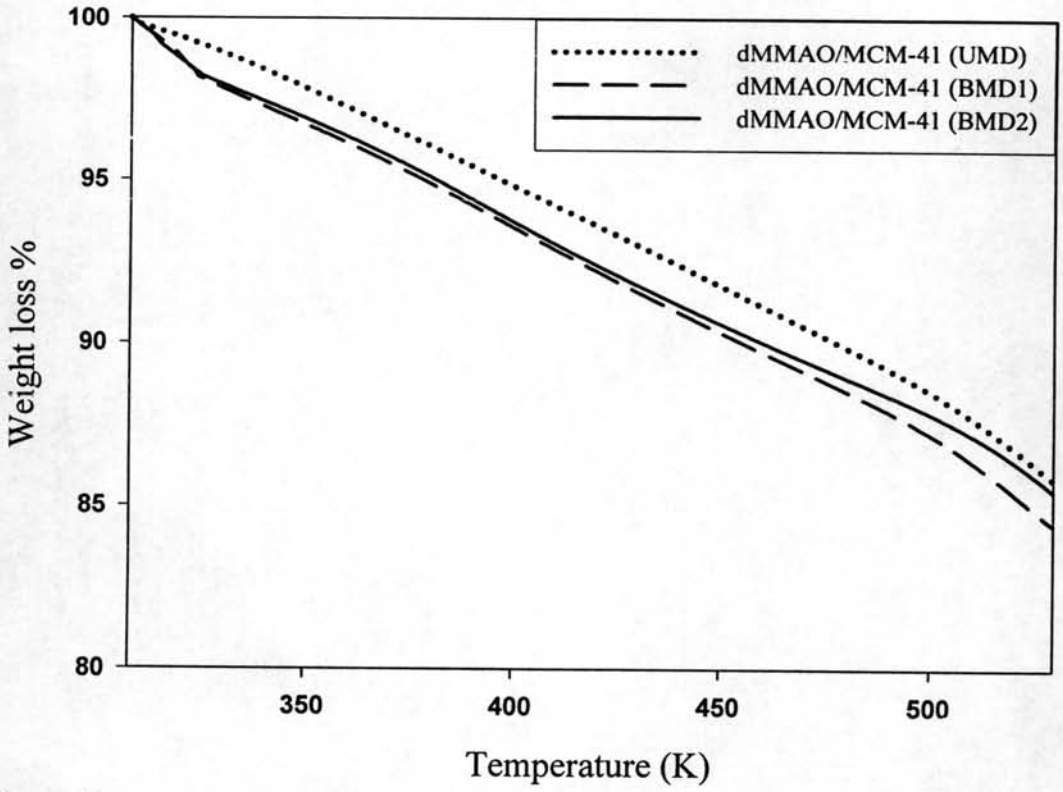
dMMAO/MCM-41 (UMD)
dMMAO/MCM-41 (BMD1)
dMMAO/MCM-41 (BMD2)
Weight loss %
100
95
90
85
80
350
400
450
500
Temperature (K)

**Figure 5**

# VITA

Miss Sirinlak Bunchongtarakarn was born on April 15, 1983 in Satun, Thailand. She received the Bachelor's Degree of Chemical Engineering from the Department of Chemical Engineering, Faculty of Engineering, Prince of Songkla University in March 2005, she continued her Master's study at Chulalongkorn University in June, 2005.